

THESIS FOR THE DEGREE OF LICENTIATE IN
SOLID AND STRUCTURAL MECHANICS

Differential railway track settlement in a transition
zone – Field measurements and numerical
simulations

KOUROSH NASROLLAHI

Department of Mechanics and Maritime Sciences
Division of Dynamics
CHALMERS UNIVERSITY OF TECHNOLOGY
Gothenburg, Sweden, 2023

Differential railway track settlement in a transition zone –
Field measurements and numerical simulations

KOUROSH NASROLLAHI

© Kourosh Nasrollahi, 2023

Thesis for the degree of Licentiate – Department of Mechanics and Maritime Sciences
2023:07

Department of Mechanics and Maritime Sciences
Chalmers University of Technology
SE-412 96 Gothenburg
Sweden
Telephone + 46 (0)31-772 1000

Cover:

Sketch of model used for simulation of dynamic vehicle–track interaction in a transition zone between ballasted track and 3MB slab track.

Chalmers Reproservice
Gothenburg, Sweden 2023

Differential railway track settlement in a transition zone – Field measurements and numerical simulations

KOUROSH NASROLLAHI

Department of Mechanics and Maritime Sciences

Chalmers University of Technology

ABSTRACT

In a transition zone between two different railway track forms, there is a discontinuity in track structure leading to a gradient in track stiffness. Examples include transitions between different superstructures, e.g., slab track to ballasted track, and/or between different substructures, e.g., embankment to a bridge or tunnel structure. Differences in loading and support conditions at the interfaces between track superstructure and substructure on either side of the transition may lead to differential track settlement and an irregularity in longitudinal rail level soon after construction because of densification of ballast and consolidation in the subsoil. This results in an amplification of the dynamic traffic loading along the transition. To ensure the safety of railway operation and reduce maintenance costs, it is necessary to monitor the condition of the transition zone and detect any operational change at an early stage.

A methodology for the simulation of long-term differential track settlement, the development of voided sleepers leading to a redistribution of rail seat loads, and the evolving irregularity in vertical track geometry at a transition between two track forms, is presented. For a prescribed traffic load, the accumulated settlement is predicted using an iterative approach. It is based on a time-domain model of vertical dynamic vehicle–track interaction to calculate the contact forces between sleepers and ballast in the short term. These are used in an empirical model to determine the long-term settlement of the ballast and subgrade below each sleeper. Gravity loads and state-dependent track conditions are accounted for. The methodology is applied to a transition zone between a ballasted track and a slab track that is subjected to heavy haul traffic. The influence of higher axle loads and the implementation of under sleeper pads on sleeper settlement is assessed.

Based on fibre Bragg grating sensors, a setup for in-situ long-term condition monitoring of track bed degradation in a transition zone has been developed and implemented to provide data for verification and calibration of the simulation model. The system is designed for measurements in an operational railway track in harsh conditions in the north of Sweden. The instrumentation along the transition comprises four clusters, each with an optical strain gauge array on the rail web in one sleeper bay, and an accelerometer and a displacement transducer on the sleeper end. Two additional accelerometers are installed far from the transition zone to measure a reference state. Combined, the data should not only provide details on long-term settlements, but also the change in dynamic response it underpins.

Keywords: Transition zone, empirical settlement model, dynamic vehicle–track interaction, non-linear track model, heavy haul traffic, 3MB slab track, fibre Bragg grating sensors, condition monitoring

PREFACE AND ACKNOWLEDGEMENTS

The work presented in this thesis was accomplished between October 2020 and April 2023 at the Division of Dynamics at the Department of Mechanics and Maritime Sciences, Chalmers University of Technology. It was performed as part of the activities within the National Centre of Excellence in Railway Mechanics CHARMEC (CHAlmers Railway MEChanics, see <https://www.charmec.chalmers.se/>) in the project TS22 – *Transition zone design for reduced track settlements*. Parts of the study have been funded from the European Union's Horizon 2020 research and innovation programme in the projects In2Track2 and In2Track3 under grant agreements Nos 826255 and 101012456. The project has been supported by CHARMEC's industrial partners. In particular, the support from Trafikverket, voestalpine Railway Systems GmbH and Abetong AB is gratefully acknowledged. Parts of the simulations were performed using resources at Chalmers Centre for Computational Science and Engineering (C3SE) provided by the Swedish National Infrastructure for Computing (SNIC).

I would like to express my sincere gratitude to my main supervisor Prof. Jens Nielsen for your endless help, guidance and support. You are always willing to help me with everything from critical thinking, interpreting results, and careful proofreading. Your pedagogical thinking will have a life-long influence on me. I would like to thank my co-supervisors Prof. Magnus Ekh and Prof. Jelke Dijkstra, and my co-author Dr Emil Aggestam, for inspiring discussions and enlightening advice. Thank you, Jelke, for guiding me into the experimental field and helping me understand how we can push models to capture real phenomena. Thank you, Magnus, for helping me to learn how to prioritize my work. Thank you, Emil, for always being available for meetings and questions regarding transition zone modelling and sharing information with me.

I would like to thank the measurement campaign members. In particular, Anders Karlsson who helped me with many brilliant mechanical solutions to make this measurement set-up working. Further, thank you, Dr Rikard Granström, Dr Matthias Asplund, Mr Carlos Hermosilla, Mr Markus Lindmark and Mr Adam Axelsson, as well as the rest of the crew during the construction of the 3MB slab track system. Special thanks to John Odowd, Aydin Zadeh and Debasish Nayak from Optics11 for teaching me about fibre Bragg gratings.

I would like to thank the members of the project reference group. The fruitful discussions with Dr Martin Li, Dr Martin Schilke, Mr Kenneth Viking and Mr Peter Zackrisson from Trafikverket, and Dr Carl Wersäll and Prof. Stefan Larsson from the Royal Institute of Technology (KTH) in Stockholm, are gratefully acknowledged. I would like to say a special thanks to Alireza Ahmadi for teaching me a lot about Discrete Element Modelling. Further, I would like to say thanks to Dr Saeed Hossein Nia and Mr Ingemar Persson for helping me validate the vehicle model.

Also, I want to thank all the friends and colleagues at the Division of Dynamics and the Division of Material and Computational Mechanics. The work would not have been the same without the great atmosphere. Furthermore, I would like to thank my late father (I admire your sacrifices for us), mother, brother and sister for always being there for me. Finally, I would like to express my deepest gratitude to my wife, Nasrin. Thank you for all the love and support you surround me with.

Gothenburg, April 2023, Kourosh Nasrollahi

THESIS

This thesis consists of an extended summary and the following appended papers:

- Paper A** Nasrollahi K, Nielsen JCO, Aggestam E, Dijkstra J, Ekh M. Prediction of long-term differential track settlement in a transition zone using an iterative approach. *Engineering Structures* 2023; 283:115830. <https://doi.org/10.1016/j.engstruct.2023.115830>.
- Paper B** Nasrollahi K, Dijkstra J, Nielsen JCO. Real-time condition monitoring of a transition zone in a railway structure using fibre Bragg grating sensors. To be submitted for international publication.

The appended papers were prepared in collaboration with the co-authors. The author of this thesis was responsible for the major progress of the work including taking part in the planning of the papers, developing the theories and the numerical implementation, data processing, instrumenting the test site, measuring, running the numerical simulations and writing the papers.

OTHER PUBLICATIONS BY THE AUTHOR

- Nasrollahi K, Nielsen JCO, Aggestam E, Dijkstra J, Ekh M. Prediction of differential track settlement in transition zones using a non-linear track model. *Advances in Dynamics of Vehicles on Roads and Tracks II: Proceedings of the 27th Symposium of the International Association of Vehicle System Dynamics, IAVSD2021, August 17–19, 2021, Saint Petersburg, Russia.*
- Nasrollahi K, Dijkstra J, Nielsen JCO, Ekh M. Long-term monitoring of settlements below a transition zone in a railway structure. *Proceedings of the 11th International Symposium on Field Monitoring in Geomechanics, ISFMG2022, September 4–7, 2022, London, United Kingdom.*

CONTENTS

Abstract	i
Preface and acknowledgements	iii
Thesis	v
Part I – Extended summary	
1 Introduction	1
1.1 Background and motivation	1
1.2 Aim of research	2
1.3 Scope and limitation	2
2 Transition zones	3
2.1 Components	3
2.2 Problems in transition zones	5
2.3 Transition zone design	6
2.3.1 Size and spacing of sleepers	7
2.3.2 Auxiliary rail	7
2.3.3 Rail pads and under sleeper pads	8
2.3.4 Sleeper material	8
2.3.5 Geocells, geotextiles, soil cement and cement gravel	9
2.3.6 Polyurethane grout technology and glued ballast	9
2.3.7 Reinforced foundations by piles and stone columns	9
2.3.8 Hot mix asphalt in trackbed layers	10
2.3.9 Embedded bridge structures	10
2.3.10 Transition wedges	11
2.3.11 Concrete confinement walls	12
3 Modelling	13
3.1 Background and introduction	13
3.2 Vehicle model	13
3.3 Track model	15
3.4 Settlement model	18
3.5 Constitutive models	22
3.6 Iterative scheme	22
3.7 Demonstration of model	23
4 Condition monitoring in transition zones	25
4.1 Background and introduction	25

4.2	3MB slab track demonstrator and transition zone	27
4.3	Fibre Bragg gratings	28
4.4	Instrumentation	30
4.4.1	Rail strain and rail bending moment	32
4.4.2	Vertical sleeper displacement and acceleration	34
4.4.3	Wheel–rail contact force	37
4.4.4	Total station	37
5	Outline of the appended papers	39
5.1	Paper A	39
5.2	Paper B	39
	References	41
	Part II – Appended Papers A – B	49

PART I – EXTENDED SUMMARY

1 Introduction

1.1 Background and motivation

In a transition zone between two different railway track forms, there is a discontinuity in track structure leading to a gradient in track stiffness. Examples include transitions between different superstructures, e.g., slab track to ballasted track, and/or between different substructures, e.g., embankment to a bridge or tunnel structure. Differences in loading and support conditions at the interfaces between track superstructure and substructure on either side of the transition may lead to differential track settlement and an irregularity in longitudinal rail level soon after construction because of densification of ballast and consolidation in the subsoil. This results in an amplification of the dynamic traffic loading along the transition, contributing to the degradation process of the foundation and resulting in a further deterioration of vertical track geometry [1–13].

To maintain smooth traffic operation, the cost for mitigating problems associated with railway transitions is often high [14–16]. For example, about \$200 millions are spent annually on track transition maintenance in the U.S. railways [11], while in Europe the cost is about \$85 millions [12]. Therefore, a thorough maintenance scheme for the railway network is essential to ensure that transition zones are adequately maintained. However, extra maintenance can be costly and may require reducing the capacity of the network. Transition zones represents an area where significant improvements might be achieved by understanding the mechanisms that are contributing to the accelerated track degradation. Research in this area will lead to an improvement of the design of new railway structures, and a more efficient maintenance of existing ones.

1.2 Aim of research

The objectives of this research are to predict and measure the long-term performance of transition zones between two track forms, and to provide guidelines for improved transition zone design. To this end, the following parts have been completed and are presented in this thesis.

- Simulation model for the prediction of long-term differential track settlement in a transition zone using an iterative approach (**Paper A**)
- Real-time condition monitoring of a transition zone in a railway structure using fibre Bragg grating sensors (**Paper B**)

The following future parts are foreseen in the second half of the project:

- Calibration of 2D and 3D track models for simulation of dynamic vehicle–track interaction and differential settlement in transition zones using field measurement data
- Guidelines for transition zone design

1.3 Scope and limitation

This multidisciplinary research project combines modelling and field measurements. It includes an extensive field test campaign and long-term condition monitoring of a transition zone in the demonstrator at Gransjö on Malmbanan used in the EU-project In2Track-3, which is part of the European Union's Horizon 2020 research and innovation programme Shift2Rail. Further, it covers numerical modelling of geotechnics and dynamic vehicle–track interaction, as well as post-processing of data. Each field requires assumptions and simplifications to reach an acceptable level of accuracy at a reasonable cost for equipment and computational effort. Some of the challenges are the difficulties to perform field measurements for data acquisition in the harsh environmental conditions at the test site, including the wide temperature range and freeze-thaw cycles in northern Sweden, that in the long-term can affect condition monitoring equipment, track properties and subgrade behaviour. Another difficulty is the operational variability in train types and axle loads.

2 Transition zones

2.1 Components

In general terms, a transition zone consists of three parts: a so-called open track on ballast, an approaching zone on ballast and an engineering structure [12], see the example in Figure 1. The open track is the part of the transition that is relatively far away and therefore unaffected by the presence of the engineering structure. The general recommendation used by the Swedish Transportation Administration is that the length of the transition zone should be at least the distance the vehicle travels during half of a second [17]. Typical lengths of transition zones are 5 – 30 metres [18]. The approaching zone is located close to the engineering structure and may suffer from severe track degradation and differential settlement in case of a poorly performing design. The engineering structure can be a bridge, culvert, tunnel, or a level crossing, or as studied in this thesis, the transition can be between a ballasted track and a ballastless/slab track.

An example of a layout of the transition zone between a ballasted track and a slab track is presented in Figure 2(a). The ballasted railway track includes several layers of geomaterials to safely transmit and distribute the train-induced load into the subgrade soil. It constitutes of two major components: superstructure and substructure. The superstructure consists of the rails, sleepers, rail pads, rail fastening systems and sometimes under sleeper pads. The substructure includes the geotechnical layers such as the ballast, sub-ballast, backfill and subgrade, whose characteristics significantly influence the track response [19], see Figure 2(b).

Traditionally, the layers of the substructure are designed using empirical and simplified theoretical approaches based on experience from in-service tracks, augmented with extensive laboratory and field test data [20,21]. These conventional design approaches may lack general applicability in different traffic load and soil conditions. This serious limitation has become more apparent with the dramatic increase in transportation needs, which has accelerated the deterioration of existing tracks and incurred significant maintenance costs. Thus, to reach optimum performance of railway tracks, including transition zones, there is an inevitable need for a more reliable, practical, and adaptable design method. The development of such a design technique requires a detailed analysis of the mechanical behaviour of both track superstructure and substructure, as well as their mutual interaction.

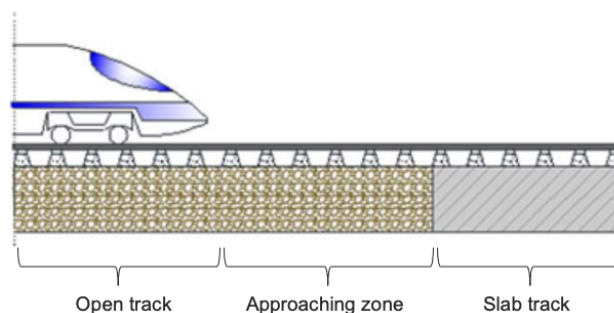


Figure 1: Schematic diagram of the different parts of a transition zone [12]

The high availability and relatively low cost of ballast makes it an ideal geomaterial for railways [5]. The ballast is formed by a layer of medium to coarse-sized aggregates (32–64 mm) of angular-shaped, uniformly graded granular material free from dust, and not prone to cementing action, [22]. It should allow for drainage and alleviation to frost, as well as adjustment of track geometry. The main function is to distribute the train loads to the underlying subsoil, to attenuate the dynamic loading and to provide lateral resistance and rapid drainage [22]. The ballast layer must ensure a uniform distribution of loads to the underlying subgrade, and its optimum thickness is usually 250 – 300 mm measured from the bottom surface of the sleepers [22].

The sub-ballast is the granular layer that is located between the ballast and the subgrade. Generally, it is placed there as a specific layer, but it may also have evolved from particle wear, densification of ballast, or old ballast layers due to decades of loading and track maintenance. The sub-ballast distributes the load and reduces stress in the subgrade depending on its stiffness and thickness. Further, this layer must be well drained and avoid positive pore water pressure under repeated loading, consist of durable, angular particles that interlock and resist abrasion, provide separation between the ballast and subgrade, and help to provide frost protection to the subgrade in cold climate [19,23].

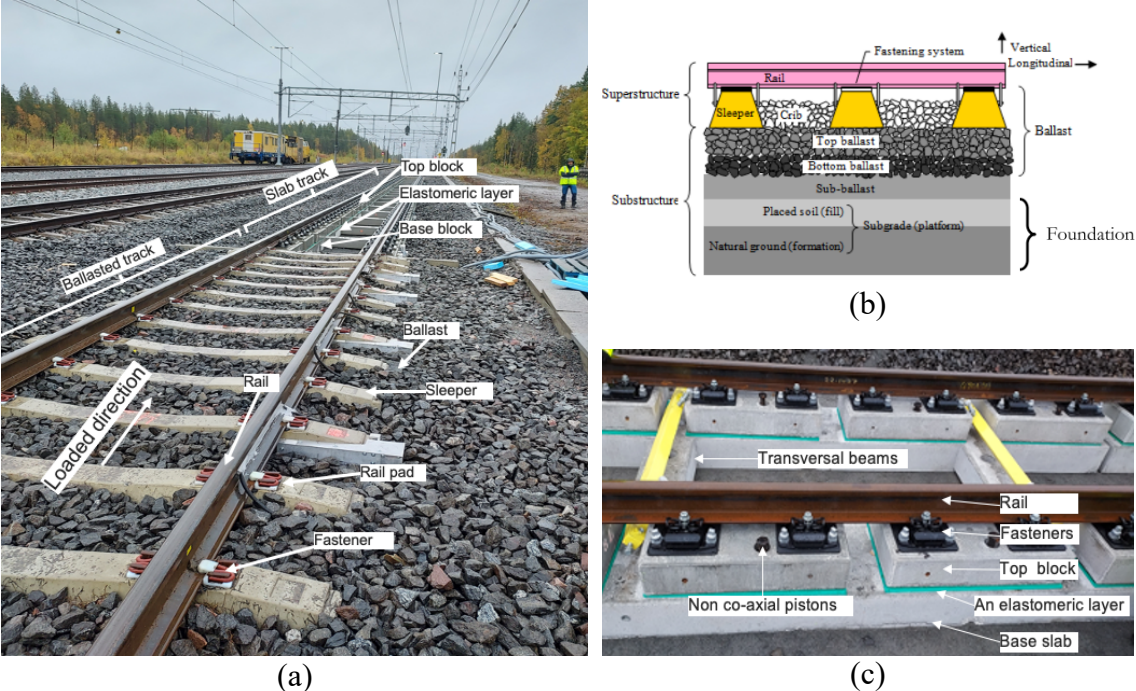


Figure 2. (a) View of transition zone between ballasted track and 3MB slab track; (b) Cross-section of ballasted track including rail, rail pads, fasteners, sleepers, ballast, sub-ballast, and subgrade [20]; (c) 3MB slab track design consisting of base slabs, top blocks, and an elastomeric layer between the concrete layers

The subgrade, which is the foundation on which everything above depends for support, is often the most variable and potentially the weakest part of the track [19,23]. It should provide a stable foundation for the sub-ballast and ballast layers. Subgrade conditions can vary over a wide range depending on the geological environment and the conditions at the construction site.

Even though ballasted track is the most common track form, modern infrastructure for high-speed railway traffic is often built using slab track [24]. Compared to ballasted track, slab track has several advantages, e.g., higher lateral track resistance and eliminated problems with ballast degradation. This reduces the need for regular maintenance and extends service life. However, should maintenance work on slab track be required, it is often more costly compared to maintenance work on ballasted track. Furthermore, there is less tolerance for corrections compared to ballasted track. Over the years, the use of optimised and prefabricated slab track systems has increased, and the initial cost ratio compared to ballasted track has been reduced [14]. For example, the “Moulded Modular Multi-Blocks slab track” (3MB) concept is a reinforced standard precast slab track designed for both mixed and high-speed traffic [25]. As part of the European Union's Horizon 2020 research and innovation programme in the projects In2Track2 and In2Track3, this particular design is being demonstrated in the field on a short section of track on the heavy haul line Malmbanan in Sweden, with tests that started in autumn 2022.

2.2 Problems in transition zones

The main problems occurring in transition zones are:

- Stiffness gradient between two different track forms leading to higher dynamic loads
- Differential track settlement and the formation of an irregularity in longitudinal rail level due to degradation mechanisms in the substructure

These problems have been addressed extensively in the literature. For example, in the review on experimental testing and modelling of transition zones by Indraratna et al. [1], the main reasons for differential settlement were hanging (voided) sleepers in the transition and difference in track stiffness on the two sides of the transition. Wang and Markine [12,26] concluded that the influence of differential settlement on track degradation is higher than the influence of stiffness variation in the transition between two track forms. Also, it has been shown that the dynamic vehicle–track interaction is different when comparing situations where traffic is moving either from a softer to a stiffer track form, or from a stiffer to a softer track form. Similar conclusions have concluded in **Paper A** and Refs. [27–33]. Further, differential settlement leads to the development of dips and bumps near the transition, which has been investigated by many researchers [34–36]. For example, in the U.S., it was found that more than 50% of all bridge transitions face dips with an average depth of 33 mm and length 5.2 m [34]. Even on well-constructed and well-maintained track, the support stiffness varies from one sleeper to the next [37]. High variability in support stiffness along the track leads to higher dynamic loads, which increase with train speed. Track stiffness needs to be sufficiently high to

provide resistance to applied traffic loads, assure track stability and bearing capacity, and reduce track deterioration. Meanwhile, track stiffness should not be too high, because then it may cause increased stresses in the track structure leading to wear and fatigue problems for track components e.g., rails and fastenings. To achieve a good design and low maintenance cost, it is commonly agreed that track stiffness and its variation needs to be kept within a certain range, ideally close to an optimum value [38–42]. In [42], it was suggested that an optimum value of vertical track stiffness at rail level for high-speed lines on ballasted track should be in the order of 90 kN/mm. Another recommended value for the vertical dynamic track stiffness is 100 kN/mm [43], which corresponds to a rail deflection of 1.0 mm under a wheel load of 100 kN. The vertical track stiffness at rail level can be defined as the ratio between the vertical wheel load exerted on the running surface of the top of the rail and the resulting vertical displacement of the rail at the same position [38].

2.3 Transition zone design

Reviews of transition zone design can be found in Sañudo et al. [10] and Indraratna et al. [1]. Available solutions to improve transition zones have been categorized in different ways. The main goal of transition zone design is to minimize the difference in track stiffness between the open track and the engineering structure. By using different distributions and properties of various elements in the superstructure or substructure, it is possible to design an appropriate gradual variation in stiffness along the transition zone. Sañudo et al. [10] used a categorization depending on the location of the structure where the design improvement is made. This includes: i) design of the substructure (subgrade), ii) design of the superstructure, and iii) mixed solutions combining i) and ii). As an alternative, Wang and Markine [26,44] separated mitigation measures for transition zones depending on their time of installation, which is either during the design stage (preventive measures) or during the operation stage (corrective measures).

In this thesis, the design solutions related to transition zones are divided into the following four categories, see also Sañudo et al. [10]. Several of the solutions are explained in more detail below.

- Mitigation of stiffness gradient in transition zone
- Improved track foundation
- Minimizing differential long-term vertical displacements between transition and engineering structure
- Combined designs

2.3.1 Size and spacing of sleepers

For a given bed modulus of the structure below the sleepers, the use of sleepers with larger base area and shorter sleeper spacing will increase track stiffness at rail level. The larger bearing area of the sleeper distributes sleeper–ballast forces more evenly over the ballast, reduces stress concentrations and prevents long-term degradation [10,45], see Figure 3.

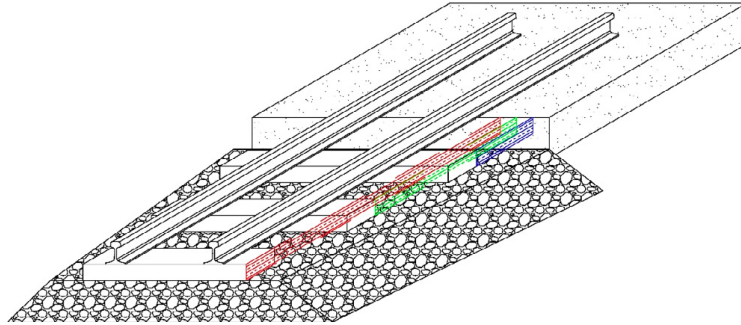


Figure 3. Variable sleeper length solution [10]

2.3.2 Auxiliary rail

Track stiffness is influenced by the implementation and number of auxiliary rails, see Figure 4. Although a limited number of studies seems to have been performed related to this solution, potential benefits have been shown. For example, Chumylen et al. [46] concluded that using two auxiliary rails in a transition zone can improve the dynamic characteristics of the track, reduce stiffness gradient and differential track settlement, and improve stress distribution in the ballasted track. Applying a wider separation of the auxiliary rails by placing them closer to each of the rails, compared to a narrow placement, offers slightly improved dynamic performance [46]. However, tamping maintenance operation with auxiliary rails is more difficult. Further, additional fastening systems and sleepers adapted to the auxiliary rails are required.



Figure 4. Sleepers adapted for two auxiliary rails in a transition zone between a ballasted track and a slab track inside a tunnel

2.3.3 Rail pads and under sleeper pads

Rail pads, see Figure 5(a), are placed between the rail and the sleeper. The use of soft rail pads reduces the transmission of high-frequency vibrations caused by wheel impacts to the ground and is the most direct method to reduce track stiffness at rail level and distribute traffic loads [6]. Under sleeper pads (USPs) are placed between sleepers and ballast, see Figure 5(b). The use of USPs pads is investigated in [2,47–50]. It provides additional damping, minimizes breakage in cracked sleepers, reduces loads between ballast particles and concrete sleepers, reduces ballast degradation, and improves passenger comfort [2,16,27,47,51]. Low stiffness USPs reduce forces acting on the substructure by improving load distribution along the track.



(a) (b)
Figure 5. (a) Rail pads, and (b) under sleeper pads [10]

2.3.4 Sleeper material

Sleepers made of composite materials, plastic material or rubber have been found to be effective in reducing the vertical track stiffness [34,52]. Nicks [34] studied the effect of using wooden, concrete or plastic sleepers on the dynamic response of a bridge approach and found that wooden sleepers help to mitigate the bumps and dips better than the other materials. However, it was also found that the wooden sleepers increase the pressure on the lower layers more than the concrete sleepers. The effectiveness of various sleeper materials in reducing track stiffness of ballasted track at the transition to a bridge was also investigated by Sasaoka et al. [16]. In their study, two methods were tested to smooth the gradient stiffness at an embankment-bridge transition: (1) replacing concrete sleepers with composite (plastic) sleepers, and (2) installing concrete sleepers on the bridge deck with thick rubber pads at the bottom of the sleepers. The vertical track stiffness measurements on the approach to, and on the decks of, bridges with three examined sleeper types (concrete, composite and concrete with rubber sleepers) were compared. It was found that both the composite sleepers and the concrete sleepers with rubber pads were successful in reducing the track stiffness measured on the approach to the bridge and the vertical track stiffness measured on the bridge.

2.3.5 Geocells, geotextiles, soil cement and cement gravel

Geocells are honeycomb-like cellular materials, where the structure is interconnected by joints to form a cellular network used for the confinement of soils. The purpose of using this technique is to reduce the risk of ballast spatter (which especially increases in transition zones) and mainly to minimize differential settlement [53].

2.3.6 Polyurethane grout technology and glued ballast

Polyurethane grout is a polymer-based material that is injected into the ground or a structure to improve its mechanical properties. This technology can be applied to address surface and cross-level track geometry issues caused by the ballast layer [54]. Jing et al. [54], reported on the application of polyurethane in transition zones. A smooth gradual track stiffness variation in a transition was achieved by using polyurethane to glue the ballast, which led to a reduced vibration of the transition zone. The application of glued ballast is shown in Figure 6. It is possible to adjust track alignment by tamping, but with the consequence that the ballast aggregates need to be reglued after the process.



Figure 6. Glued ballast [55]

2.3.7 Reinforced foundations by piles and stone columns

There is a wide variety of soil reinforcement techniques. In all these techniques, the reinforcement elements (consisting of stone, concrete, or geosynthetics) are inserted to improve the selected property of the in-situ weak soil. A review of technologies to mitigate problems in transition zones is summarized in [53]. These are stone columns, compacted columns, driven columns, geopiers, deep soil mixing (by injecting grout through augers that mix in with the soil, forming in-place soil-cement columns), concrete injected columns, continuous flight auger cast piles (CFA). Using piles or stone columns, see Figure 7, increase support stiffness and reduce deformation with almost zero settlement of the foundation, but this system is an expensive solution and needs heavy machinery [10].

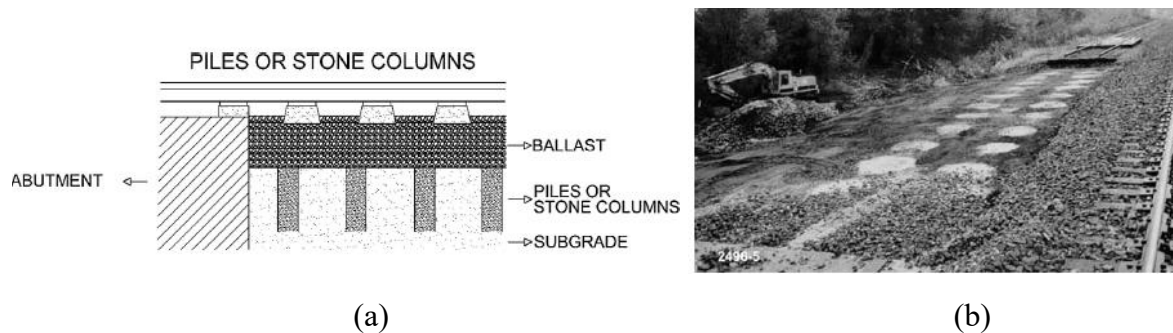


Figure 7. (a) Piles concept solution in a transition zone, and (b) stone columns installed in the subgrade [10]

2.3.8 Hot mix asphalt in trackbed layers

A layer of hot mix asphalt under the ballast reinforces weak subgrade, see Figure 8. It has been shown that this solution can reduce stresses in the subgrade and increase its load bearing capacity. In addition, it can increase vertical track stiffness and track life, and improve track drainage [55].

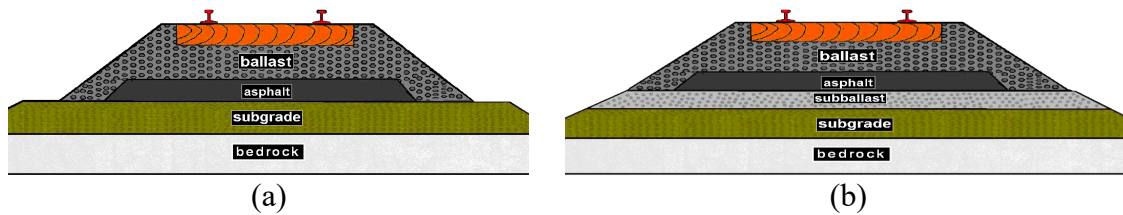


Figure 8. A sketch of asphalt underlayment; (a) without granular sub-ballast layer (common in the U.S.A.), (b) trackbed containing both asphalt and sub-ballast layers (common in the EU and Asia). From [55]

2.3.9 Embedded bridge structures

Approach slabs are usually reinforced concrete beams that can be horizontal or inclined, see Figure 9. With this technique, the depth of the ballast is gradually reduced on the approach to the engineering structure. As concluded in [56], the effectiveness of this solution relies on the fact that both dynamic track movements and long-term settlements are mainly governed by the depth of the ballast, i.e., the contribution of the subgrade to the stiffness and settlement is of minor importance. For soft subgrade, this design method can smooth stiffness gradient in a transition zone [57]. However, the inclination of the buried slab can increase over time because of long-term degradation and settlement of the embankment and subgrade.

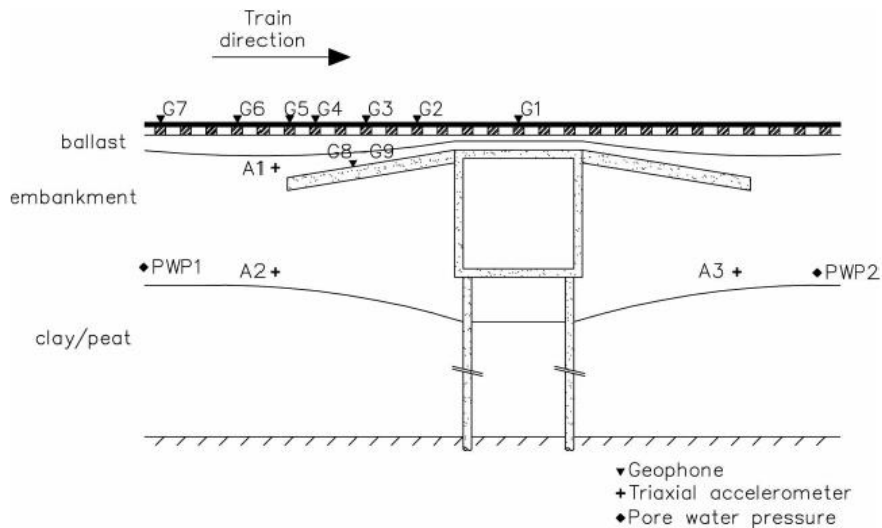


Figure 9. Typical section of an inclined transition slab. From [56]

2.3.10 Transition wedges

Transition wedges are gradual transitions (typically 20 m in length) in the backfill from softer material to stiffer material by using a bed of (bound or unbound) granular materials and granular aggregates, see Figure 10, [56,58]. Differential settlement in a transition can be reduced and the gradual transition of vertical stiffness between the two structures can be smoother. However, the wedge shape fill materials and the construction process of wedges need to meet strict performance requirements because the consequences of any malfunction will lead to high repair costs as well as traffic disruptions.

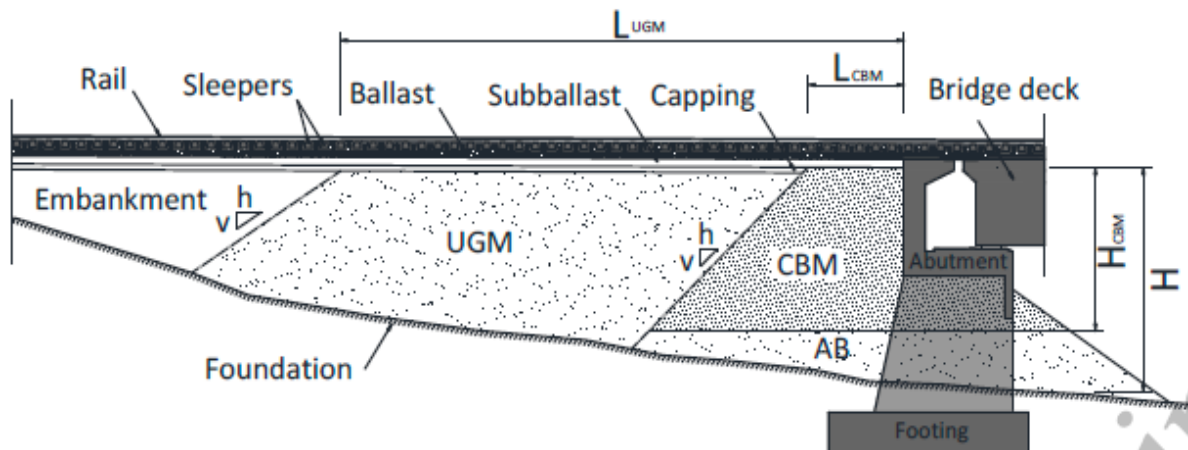


Figure 10. Sketch of transition zone design with wedge-shaped backfill. The backfill consists of a wedge with layers of Cement Bound Granular mixtures (CBM), a wedge with layers of Unbound Granular Material (UGM), and an Abutment Backfill base (AB) under the wedge-shaped CBM [59]

2.3.11 Concrete confinement walls

Concrete confinement walls (wing walls) are designed to confine the ballast and subgrade layers to provide stability for those layers. They can be installed along the transition to prevent ballast flow-down, to increase lateral confinement on ballast and hence reduce the track deformation, as well as, long-term track settlement, see Figure 11, [60]. However, this technique leads to higher vertical track stiffness resulting in ballast breakage.



Figure 11. Bridge transition zone with concrete confinement wings walls parallel to the track.
From [60]

3 Modelling

3.1 Background and introduction

Long-term settlement of transition zones has been studied extensively in the literature. Two approaches to model and predict track settlement have been suggested. One approach involves either a three-dimensional finite element (3D FE) (continuum scale) model, incorporating yield criteria, plastic flow rules, and hardening rules, or a discrete element (DE) model framework to simulate the local deformations and stresses in the substructure [8,12,21,33,61,62]. The alternative approach is using a simplified one-dimensional Winkler type model coupled with empirical models to predict settlement [31]. Such empirical formulae are typically based on cyclic triaxial test data, reduced-scale models [63] or in-situ measurements. Reviews of existing mechanistic-empirical settlement formulae can be found in Refs. [21,64,65].

Finite element models have been used extensively to perform dynamic structural analysis and simulate the effects caused by the passage of trains in transition zones. Obviously, the type of model and the modelling software/program influence how reliable and accurate is the analysis of the dynamic vehicle-track interaction. Various assumptions need to be considered in a model: the type of the required analysis (static or dynamic), linear or non-linear analysis (for example material plasticity), computational cost, and the expected outputs. An extensive review on models of dynamic vehicle-track interaction in transition zones and its applications can be found in [1,10]. Based on the type of analysis and expected output, the number of considered layers of the foundation varies in the model. Examples of track models involving one-layer models, two-layer models with elastic/rigid sleepers, and three-layer models with sleepers and ballast masses used in simulations of dynamic vehicle-track interaction are reported in Refs. [66–69].

3.2 Vehicle model

The traffic loading has been simulated using two main approaches: moving point loads with prescribed magnitudes or more advanced vehicle models based on multiple bodies (masses, springs and dampers). The simplest representation of track loading is a static load applied at a specific position [70]. However, this simplification cannot follow the nature of changing load over time. An impulse or transient force using a Dirac delta function have been considered [66]. An extension of this method is a moving point load, where the force is defined using a moving frame of reference that relates to space and time through the vehicle velocity [66]. To consider a harmonic vehicle load, a complex-valued exponential function has been applied [66,71]. However, despite allowing for an oscillating and moving representation of the excitation source, quasi-static point load models with prescribed magnitudes are significant simplifications of the aspects of loading induced by train dynamics.

Instead, the vehicle can be represented by a multi-body dynamics model. In this approach the wheelsets, bogie frames, and car body are described as rigid masses, while springs and dampers are used to model the primary and secondary suspensions. The vehicle can for example be modelled as a quarter-car model with two degrees of freedom (DOFs) representing the vertical displacements of one wheelset and half of the bogie frame, respectively. Alternatively, a half-car model can be applied with two DOFs representing the vertical displacements of the two wheelsets in a bogie and two DOFs representing the vertical displacement and rotation of the bogie frame. The model in Figure 12 is a representation of a full vehicle with car body and two bogies, see [4,6,12,44,70].

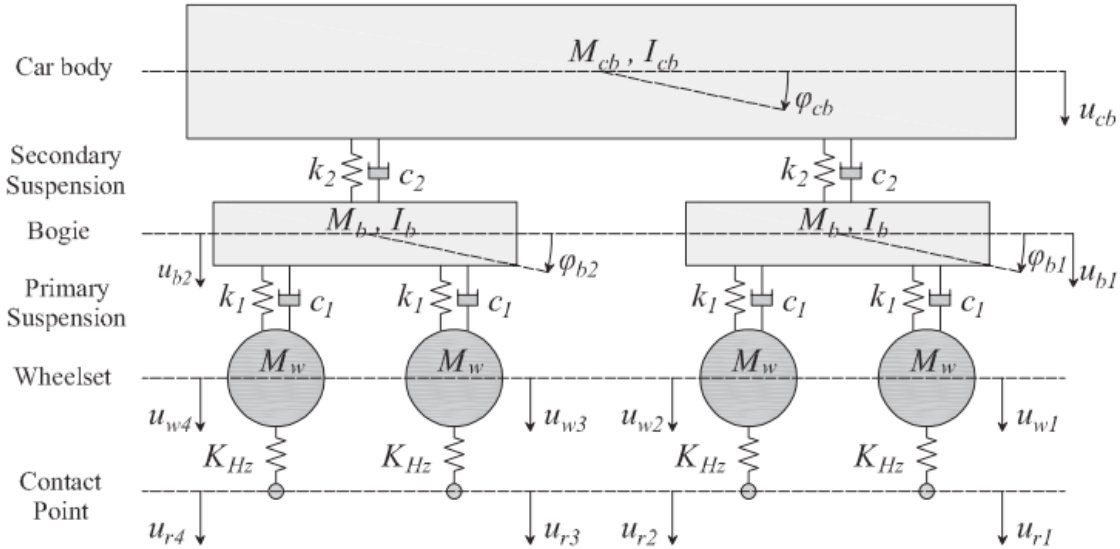


Figure 12. Vehicle model with ten degrees of freedom consisting of a car body, two bogie frames and four wheelsets [68]

The iron ore wagon used for heavy haul traffic on Malmbanan includes one car body and two three-piece bogies, each consisting of a bolster, two side frames and two wheelsets. The vehicle model used in **Paper A**, see Figure 13, has 14 DOFs, where two of the DOFs represent the motion (vertical displacement and pitch rotation) of the car body, four DOFs represent the corresponding displacements and rotations of the side frames (two DOFs per bogie), four DOFs the vertical displacement of the four wheelsets, while the four remaining massless DOFs (one per wheelset) are interfacing the rail and are used in the formulation of the constraint equations [69]. The unsprung mass of each wheelset is denoted M_w . Further, M_{bog} and J_{bog} are the mass and mass moment of inertia for each of the two side frames, while M_c and J_c are the mass and mass moment of inertia for the car body (including two bolsters). The axle distance within a bogie is Δ_w , while the bogie centre distance is Δ_{bog} . The vehicle model also includes the primary suspension stiffness k_1 and viscous damping c_1 , and secondary suspension stiffness k_2 and viscous damping c_2 . For traffic on tangent track, it is assumed that the car body and bolster are rigidly connected. Each wheelset is connected to the rail via a Hertzian contact spring.

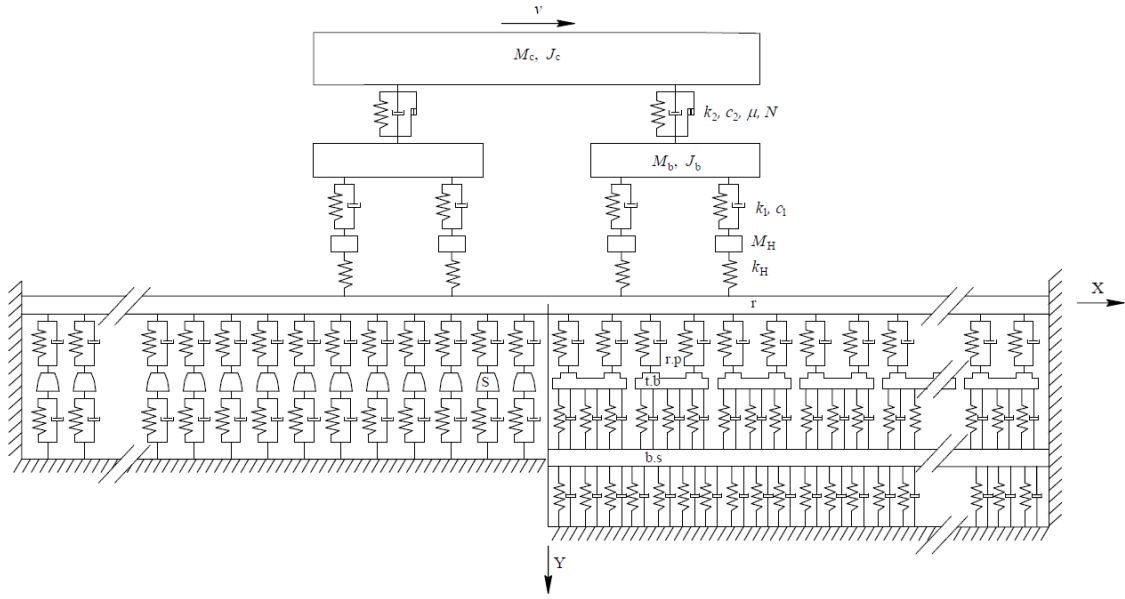


Figure 13. Sketch of complete vehicle and transition zone model. The track model contains rail (r), top blocks (t.b) and base slab (b.s) modelled by beam elements. The base slab is supported by a Winkler foundation. The sleepers (s) are rigid masses supported by a spring-damper connection (representing the ballast/subgrade) with non-linear, and potentially random, stiffness properties. From **Paper A**

3.3 Track model

The modelling of a transition zone can be achieved in various ways. In [72], the influences of settlement, variations in the foundation stiffness and vehicle speed on the vertical dynamic wheel–rail contact forces were investigated using a 2D FE model, and it was concluded that permanent differential settlement (modelled by updating the longitudinal level of the rail) is the main source of increased wheel–rail contact forces. However, this study considered only a ballasted track model and the influence of a transition zone was solely modelled by introducing a prescribed variation in rail level and/or foundation stiffness. Aggestam and Nielsen [6] presented a time-domain 2D model for simulation of vertical dynamic vehicle–track interaction in a transition between ballasted track and slab track using an extended state-space vector approach. Then, by solving a multi-objective optimisation problem using a genetic algorithm, the maximum dynamic loads on the track structure were minimised. It was concluded that the transition zone that had been optimised with respect to both directions of travel resulted in similar dynamic loads as the transition zone which only had been optimised with respect to single-direction traffic.

Grossoni et al. [2] presented an iterative methodology that couple models of vehicle–track dynamics and long-term track settlement. The substructure dynamic characteristics are modelled by using an equivalent Lumped Parameter (LP) model whose parameters are tuned

Ramos et al [5] studied the short- and long-term behaviour of ballasted and slab tracks subjected to cyclic loading. Settlement of both track forms were compared using laboratory experiments and calibrated numerical models. The two track forms were subjected to three million cycles of loading using an iterative approach. The calculated settlements were used to develop and calibrate the short-term response of 3D FE models of both track structures. In [4], the same 3D FE model integrated with an empirical settlement model was used to analyse a transition zone between slab track on an embankment and slab track in a tunnel. Contact elements were used to simulate voids between the slab's hydraulically bound layer and the frost protection layer. In each iteration, the calculated 3D stress field in the substructure is used as input in the settlement model to compute settlement along the transition. These settlements are used to modify the 3D model geometry in the subsequent iteration.

Another approach to simulate the complex degradation behaviour of the ballast layer is to use a discrete element model, see [73]. Because of the extreme computational effort to predict the interaction between each individual ballast particle, the length of the track model needs to be limited to a few sleepers [74]. The simulation results clearly highlighted the significance of particle breakage in the accumulation of permanent ballast deformation under cyclic loading. Most of the particle breakage and the highest rate of permanent strain accumulation were observed to occur during the initial load cycles. The degradation rate gradually decreased with increasing number of load cycles. In [75], a bridge–embankment transition zone model was established by combining the discrete element method (DEM) with the finite difference method (FDM), see Figure 16. In this model, the DEM was used to model sleepers and ballast particles with complex shapes, while the FDM was applied to simulate the abutment, transition section and embankment.

Coelho [76] predicted track settlement on a network scale by considering the effects of stochastic variations in traffic and soil conditions. A semi-analytical, frequency-domain cone model [77] based on the solution of a 1D wave propagation problem was applied to determine the dynamic stiffness and damping of the soil. A similar approach is used in **Paper A** to calculate the force-displacement relationship for the ballast and subgrade under a sleeper.

In **Paper A**, a methodology for the simulation of long-term differential track settlement, the development of voided sleepers leading to a redistribution of rail seat loads, and the evolving irregularity in vertical track geometry at a transition between two track forms, is presented. For a prescribed traffic load, the accumulated settlement is predicted using an iterative approach. It is based on a 2D time-domain model of vertical dynamic vehicle–track interaction to calculate the contact forces between sleepers and ballast in the short-term. These are used in an empirical model to determine the long-term settlement of the ballast/subgrade below each sleeper. Gravity loads and state-dependent track conditions are accounted for, including a prescribed variation of non-linear stiffness of the supporting foundation along the track model. Analyses of the influence of higher axle loads and the implementation of under sleeper pads on sleeper settlement are demonstrated. The applied model for simulation of dynamic vehicle–track interaction on ballasted track was originally developed by Nielsen and Igeland [69], and recently extended to slab track in [24].

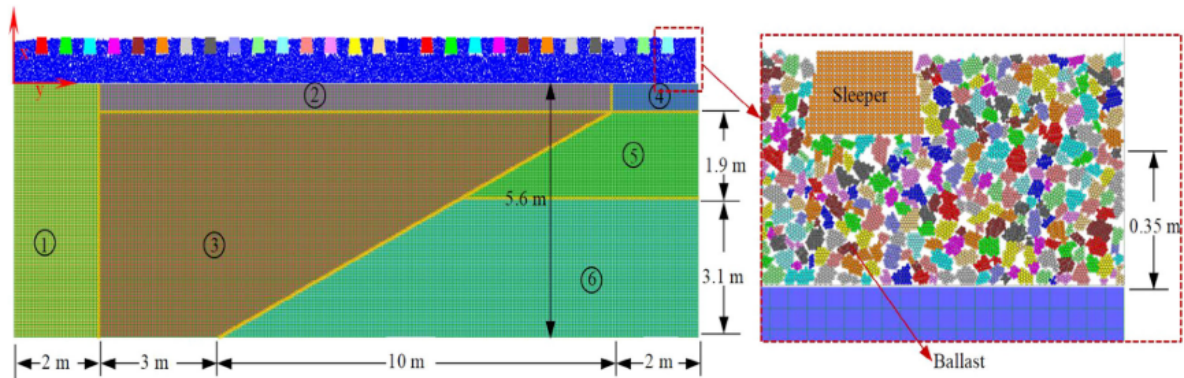


Figure 16. Coupled DEM/FDM model of a bridge–embankment transition with a wedge-shaped backfill design: 1) abutment, 2) surface layer of subgrade for transition, 3) wedge-shaped backfill, 4) surface layer of the subgrade, 5) bottom layer of the subgrade, 6) subgrade body. From [75]

3.4 Settlement model

Railway track is subjected to dynamic traffic loading due to trains at different speeds and axle loads. The cyclic loading leads to a time-variant vertical deformation of the track. A small part of this deformation will be permanent meaning that after a train has passed a given section of the track, the track does not return to its position from before the train arrived. These small permanent deformations accumulate over the large number of loading cycles during the life of the track and may lead to large permanent differential settlement affecting track geometry. For example, a granular aggregate (such as ballast) subjected to cyclic loading will densify and hence reduce its void ratio as particles glide past each other and reassemble into a new physical condition [78]. According to Refs. [22,79], higher dynamic loads at the transition induced by a gradient in vertical track stiffness and/or an initial misalignment in rail level are the major causes of the track deterioration due to differential ballast settlement. As a consequence of differential settlement, track geometry irregularities evolve and cause alterations in the distribution of loads [80]. The rate of differential settlement depends on several factors, such as the type and amount of traffic (e.g., axle load, train speed, dynamic vehicle–track interaction, accumulated traffic load), the design of the superstructure (rail and sleeper type, sleeper spacing, stiffness of rail pads and any additional resilient layers like USPs that influence the distribution of load on ballast and subgrade), properties of the layered substructure (depth, density, stiffness or resilient modulus, ballast specification in terms of particle size distribution and mineralogy, ballast contamination, drainage and pore water pressure conditions).

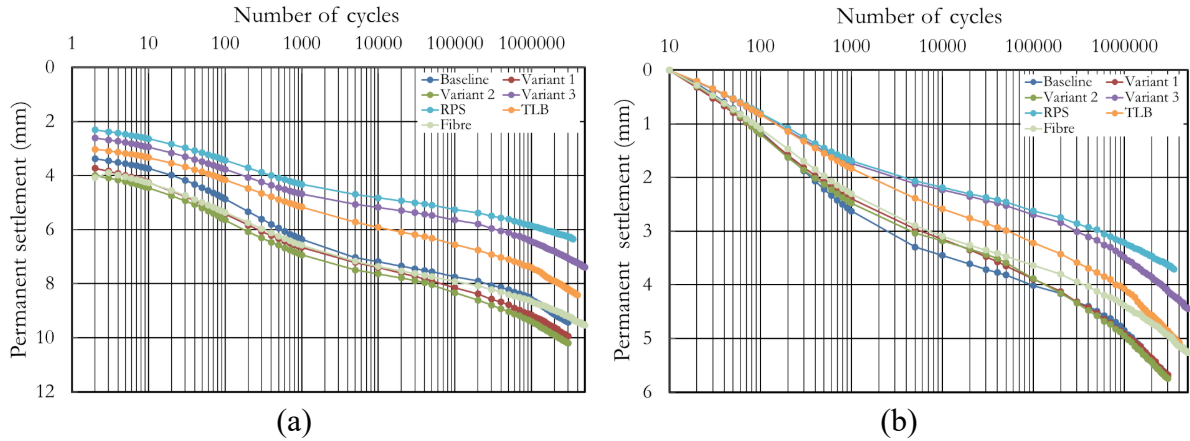


Figure 17. Permanent settlement vs. number of loading cycles, (a) of each sleeper intervention test, and (b) of each sleeper intervention test relative to the settlement after 10 loading cycles. From [81]

Extensive reviews of settlement models have been presented by Dahlberg [21], Abadi et al. [64], and Grosioni et al. [65]. Dahlberg [21] concluded that the magnitude of track settlement depends on the quality and behaviour of the ballast, sub-ballast and subgrade, and that there are two basic phases of settlement. The first phase corresponds to a higher settlement rate soon after construction of the line or after maintenance tamping, while the second phase is at a slower settlement rate that generally decreases with accumulation of traffic load. The initial phase of ballast settlement can be attributed to ballast compaction. After the ballast achieves a higher density, the second phase of ballast settlement begins to dominate. This second phase of settlement may be characterized by particle damage/fracture and further particle rearrangement. It is controlled by several factors including deviatoric stresses, vibrations, degradation and subgrade stiffness [21,64,82–84].

Empirical equations have been used to quantify and characterise track settlement. These equations have two main forms: logarithmic [79] and exponential [85]. The settlement is calculated as a function of the number of load cycles and the settlement after the first load cycle. In tests conducted up to millions of load cycles, measured track settlement vs. number of load cycles has generally shown the phases previously identified by Sato [86] and Dahlberg [21], and two inflexion points as indicated in Figure 17, [87]. To improve the fit with experimental data, more complex empirical equations have been introduced [87].

Sato [86] presented an empirical equation where settlement is a function of the number of load cycles N and the sleeper–ballast pressure P or sleeper–ballast force F , see Eq. 1. The settlement S_N depends on whether the sleeper–ballast stress exceeds a threshold stress P_{th} .

$$S_N = a \cdot (P - P_{th})^2 \quad \text{if } P > P_{th} \quad \text{Eq. 1}$$

Thus, when the pressure P is larger than P_{th} , the track settlement is proportional to the square of the difference between the sleeper–ballast pressure P and the threshold value P_{th} . In the model extended by Dahlberg [21], the power 2 was replaced by n . Based on tuning the model versus laboratory tests, and for the investigated range of pressures P , a better fit was obtained for n in

the range of 4 – 5. It was suggested that different degradation or failure mechanisms are involved in different loading ranges.

The settlement model (threshold function) used in **Paper A** is similar to the one suggested by Sato [86], and extended by Dahlberg [21], in the sense that there is no accumulation of permanent ballast/subgrade deformation if the maximum sleeper–ballast contact force generated by a passing wheel is below a certain threshold value. Furthermore, it is assumed that the model provides the permanent deformation accounting for all the layers of the substructure.

In **Paper A**, after solving the short-term dynamic vehicle–track interaction, the time history of each sleeper–ballast force is calculated in a post-processing step using the FE model of the track. For each vehicle model passage in iteration step j ($j = 1, 2, \dots, n_s$), the incremental settlement $\delta_{i,j}$ [m] at sleeper i ($i = 1, 2, \dots, N_{\text{bays}}-1$) is formulated as a function of the maxima of the sleeper–ballast contact force $F_{s/b,i}$

$$\delta_{i,j} = \sum_{n=1}^{N_w} \left\{ \sum_{k=1}^{N_k} \alpha_k \left[\frac{\langle \max (F_{s/b,i})_n - F_{\text{th},i} \rangle}{F_0} \right]^{\beta_k} \right\} \quad \text{Eq. 2}$$

where N_w is the number of wheels in the vehicle model. Within each iteration step, it is assumed that the set of $\max (F_{s/b,i})$ remains the same for all vehicle passes such that a linear extrapolation of the settlement increment to represent up to 10^5 load cycles can be carried out, see below. The order N_k of the polynomial formulation and the corresponding parameters α_k and β_k are empirical, while $F_0 = 1$ kN is a reference contact force with a unit such that the term within the square brackets becomes non-dimensional. Again, it is assumed that the model provides the permanent deformation accounting for all the layers of the substructure.

The accumulated settlement at sleeper i after n_s iteration steps (corresponding to N_s wheel passings) is calculated by summing the incremental settlements calculated for each preceding step j as

$$\Delta_i(n_s) = \sum_{j=1}^{n_s} \delta_{i,j} \quad \text{Eq. 3}$$

In the next iteration step, the accumulated settlements are applied in the updated track model. For each sleeper i , it is assumed that the current threshold value $F_{\text{th},i}$ is dependent on the accumulated settlement Δ_i as:

$$F_{\text{th},i}(\Delta_i) = F_{\text{th},\infty} - (F_{\text{th},\infty} - F_{\text{th},0})e^{-\gamma\Delta_i} \quad \text{Eq. 4}$$

where $F_{\text{th},0}$ is the virgin threshold value before any traffic loading has been applied, $F_{\text{th},\infty}$ is the long-term threshold value corresponding to a completely stabilised (consolidated) track, while γ is a parameter that determines the rate of hardening. As inspired by a visco-plastic material mechanics formulation, the threshold value is dependent on the accumulated settlement. This leads to a non-linear hardening (increase) of the threshold value with increasing settlement, see Fig. 18(a), and consequently to a decreasing settlement rate with increasing accumulated traffic

load. The parameters of the threshold value are track site specific. Thus, in future work, these parameters (as well as α_k and β_k) need to be calibrated against field measurements.

In each iteration step, up to 10^5 load cycles (corresponding to 3 MGT of traffic with loaded iron ore trains) are considered. However, an adaptive step length is applied such that the maximum allowed settlement increment δ^{\max} per iteration step is limited. If the increment exceeds δ^{\max} , a linear interpolation is applied. A convergence study on the influence of the settlement increment per iteration step on the accumulated settlement was presented in [31], and it was concluded that $\delta^{\max} = 0.2$ mm provides a reasonable compromise between accuracy and computational cost.

A similar approach but using a semi-analytical approach for the estimation of evolving track irregularities due to differential ballast settlement, is proposed by Grossoni et al. [2]. This model is based on the behaviour of granular material subjected to cyclic loading. It is able to reproduce the accumulation of plastic settlement with each load cycle, with the amount of plastic settlement per cycle related to the stress in excess of a threshold stress. The threshold stress increases with the number of load cycles (work hardening), and with the initial stiffness of the track bed, see Figure 18(b).

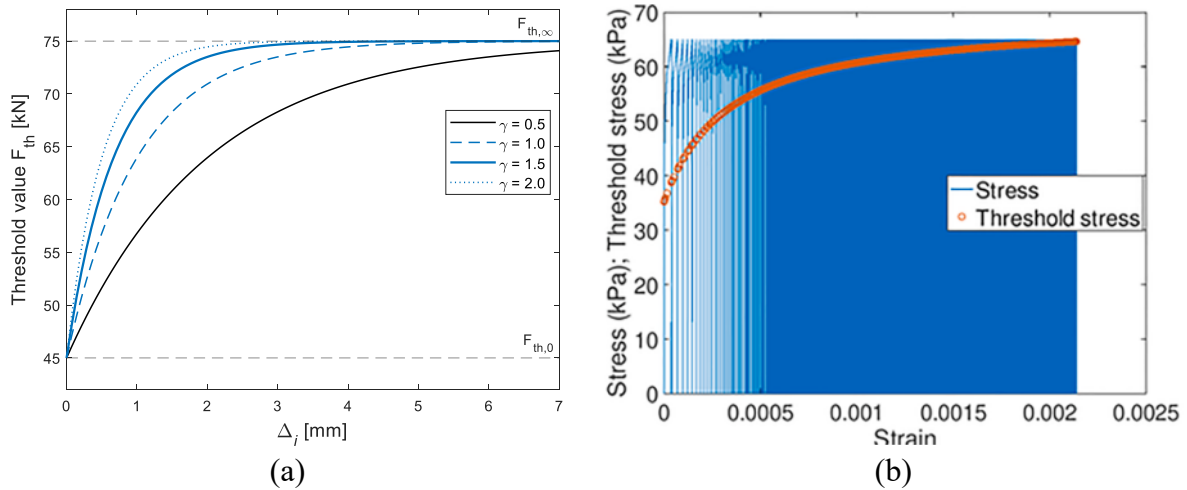


Figure 18. (a) Influence of hardening parameter γ and accumulated settlement Δ_i on threshold value F_{th} (here: $F_{th,0} = 45$ kN and $F_{th,\infty} = 75$ kN). From **Paper A**. (b) Evolution of threshold stress in a calculation using a semi-analytical model. From [2]

3.5 Constitutive models

Constitutive models accounting for the complex elastoplastic behaviour of geomaterials have been implemented in 2D and 3D FE models but are generally associated with a higher computational cost, see e.g., [4,11,32,59]. The most widely used model to describe the non-linear stress dependent stiffness of unbound granular materials (such as ballast) is the $K - \Theta$ model, or power law model, see [61,88]. Compared with using a constitutive model, results from empirical models have been reported to be similar in accuracy yet depending on a much smaller number of input parameters [4].

3.6 Iterative scheme

To simulate the settlement increment induced by each passing vehicle, or even each passing wheel, would require a high computational cost. A common technique to address this problem is to use an integrated approach where a model of the dynamic vehicle–track interaction in the short term is combined with an empirical model of the long-term settlement. For example, Sayeed and Shahin [89] considered the effect of a moving dynamic vehicle load and applied a 3D FE model to compute the deviatoric stresses in the foundation that were then used as input in an empirical settlement model. A cyclic domain model integrated with an iterative approach to compute differential track settlement while accounting for longitudinal variations in load and track properties was developed by Li et al. [32]. Similar techniques have been used to predict settlement in transition zones, see [4,11,12,29].

The simulation model applied in **Paper A** is based on an iterative approach where a time-domain model of vertical dynamic vehicle–track interaction in the short term (accounting for voided sleepers and state-dependent properties of the ballast and subgrade at each sleeper–ballast interface) is integrated with an empirical model of accumulated ballast and subgrade settlement in the long term, see also [31]. The simulation procedure is illustrated in Figure 19. In each iteration step, one time-domain simulation of short-term vehicle–track dynamics is performed, where the pre-calculated static track displacement due to gravity load is used as initial conditions. The calculated load maxima at the interface between each sleeper and ballast in the ballasted track section, generated by the combination of gravity load and each of the passing wheels of the vehicle model, are identified and used as input to an empirical settlement model. In each iteration step, the track model is updated to account for the current states of the support conditions, and it is assumed that the same set of load maxima is generated by all passing vehicles. By taking several iteration steps, the accumulated differential settlement in the long term, the potential development of voided sleepers and the resulting redistribution of foundation loads between adjacent sleepers are calculated.

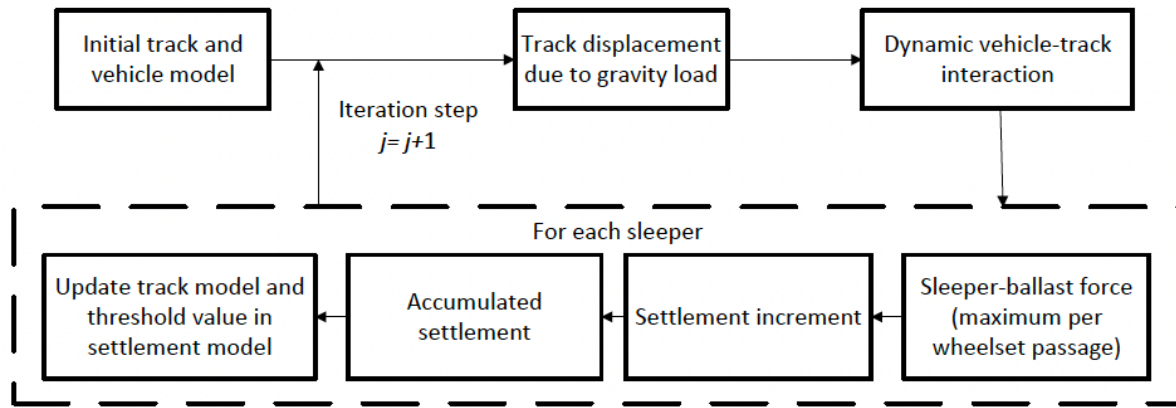
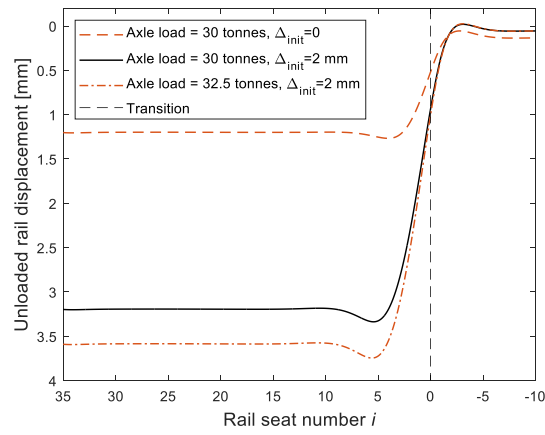


Figure 19. Iterative procedure to predict differential settlement in a transition zone. From **Paper A**

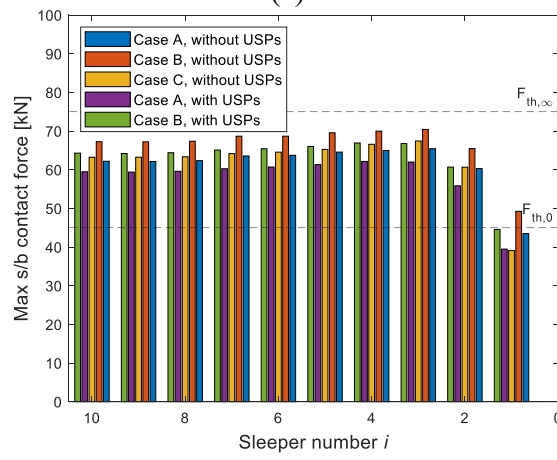
3.7 Demonstration of model

To demonstrate the model presented in this thesis, a few results from the iterative calculation procedure are presented below. An initial vertical misalignment Δ_{init} in rail level between the two track forms is assumed for some of the calculated cases. The predicted rail displacement due to gravity load and due to the accumulated sleeper settlement after a traffic load of 45 MGT is shown in Figure 20(a). For the same level of initial misalignment, it is observed that an increase of axle load leads to a considerable increase of settlement, both in terms of a higher uniform settlement away from the transition and a larger local maximum (dip) near the transition. Based on the depth of the dip near the transition relative to the uniform settlement, it can be concluded that the stiffness gradient at the transition leads to a minor contribution to the unloaded rail displacement, while the influence of the initial misalignment is more significant.

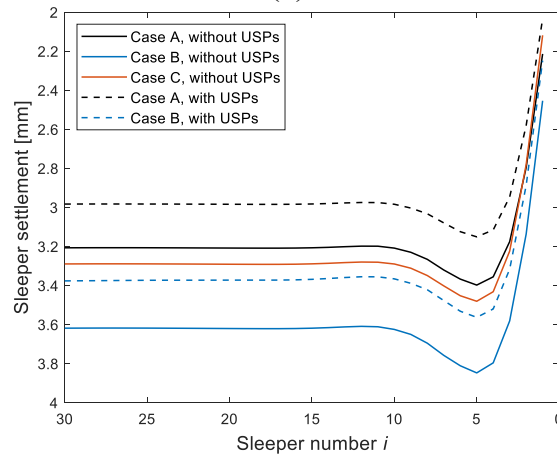
As discussed above, the use of USPs reduces the track stiffness at rail level and leads to a wider distribution of load along the sleepers and along the track. The influence of implementing USPs on the maximum sleeper–ballast contact force at the transition after one iteration is illustrated in Figure 20(b). As expected, it can be observed that the USPs lead to lower sleeper–ballast contact forces. For all cases illustrated in Figure 20(b), sleeper–ballast contact forces are higher for Sleepers 3 – 7 than elsewhere, and the maximum sleeper–ballast contact force exceeds the initial threshold value for all sleepers except Sleeper 1 (except for the case with the linear model of sleeper support stiffness, axle load 32.5 tonnes and without USPs). This explains the evolution of the local maximum in differential settlement near the transition. It is also observed that the accumulated settlement is reduced by implementing USPs, see Figure 20(c). For a further demonstration of the model and a continued discussion of the results, see **Paper A**.



(a)



(b)



(c)

Figure 20. (a) Influence of axle load and initial misalignment Δ_{init} on rail displacement due to gravity load after an accumulated traffic load of 45 MGT. (b) Maximum sleeper–ballast contact force along the transition zone in the first iteration. (c) Accumulated settlement per sleeper along the transition zone after 45 MGT. From **Paper A**

4 Condition monitoring in transition zones

4.1 Background and introduction

Several field investigations have been carried out to evaluate the performance of transition zones and to monitor the differential settlement. Various instruments and sensors have been used to measure the track response in real time scenarios. This includes multi-depth deflectometers, uniaxial and triaxial accelerometers, strain gauges, pressure cells, settlement pegs, video gauge systems, position sensitive devices, geophones, inclinometers, linear variable displacement transducers, among others. In this section, some previous experimental research is reviewed.

Coelho [26] presented the results from an extensive monitoring campaign of transition zones (embankment-culvert) in the Netherlands. The monitoring program included both dynamic measurements due to regular train passages, and static measurements. Four metre long and 300 mm thick approach slabs were used on both sides of the culvert. The gap above the approach slab was filled with sand up to the ballast under the actual track. The vertical displacement at different depths of ballast and subgrade, axle load, and average track stiffness were measured using geophones (mounted on top of wooden sleepers), uniaxial accelerometers (within the ballast), triaxial accelerometers (within the soil below track), strain gauges and a high-speed camera [26]. It was concluded that voided sleepers in the transition zone due to long-term differential track settlement were the main sources of the large track displacements that caused increased impact loading and accelerated track degradation. Fortunato et al. [44] investigated a wedge-shaped approach slab in a transition zone and concluded that a gradual transition of vertical stiffness can be achieved with this approach.

Structural health monitoring of rail tracks and transition zones can be carried out using conventional track geometry cars and other advanced techniques, such as digital image correlation (DIC) and satellite synthetic aperture radar (InSAR) systems. In Wang et al. [26], dynamic rail displacements at multiple points in transition zones were measured without track possession, providing the dynamic displacement profile of the transition zone. It was concluded that permanent rail displacements near the bridge were larger than elsewhere in transitions.

In [90], a track deflection and stiffness survey was carried out using micro-electro-mechanical-systems (MEMS) accelerometers. About 80 of these devices were placed on successive sleeper ends, primarily on the field side of the track, and then moved along the site during consecutive night-time possessions. This was done in two batches of 200 sleepers with an overlap of 50 sleeper ends, approximately measurements were repeated three months apart. The devices were programmed to record continuously at 400 Hz. The acceleration signals were filtered and integrated twice to reconstruct displacements, using 4th-order high- and low-pass Butterworth filters with cut-on and cut-off frequencies of 2 and 40 Hz, respectively [37]. Further, a webcam mounted on a telescope was positioned at 6 m from the track to reduce the influence of vibration of the ground. It captured an image of the target, which was mounted on the sleeper for the measurement of peak-to-peak displacement. However, a key limitation of this method was that

the video recording system could monitor the displacement of only one or two sleepers at a time. Also, this measurement can be inaccurate depending on train speed. The frequencies dominating the dynamic track response during the passage of trains varies depending on the bogie spacing and train speed. Thus, when a dominating frequency is over a certain value, the result can be underestimated due to the low acquisition rate of the camera. For high-speed train operation, a higher FPS is required, such as 150 Hz frame rate.

In this thesis, to investigate the performance of a selected transition zone on the Swedish iron ore line, a monitoring program was defined that comprised both long- and short-term condition monitoring. The long-term measurements focused on the static behaviour of the track. The goal was to evaluate the influence of the accumulated loading on the degradation of the transition zone. The short-term measurements concentrated on the dynamic response of the track during the passage of several types of trains. The objective was to assess the structural response when submitted to standard loading conditions, and evaluate the influence of several parameters, such as train speed and higher axle loads. In condition monitoring of a transition zone, the measurements should be undertaken with only minimal disturbance to traffic operation. Therefore, for the most part, the transition zone has been studied using trackside measurement systems.

4.2 3MB slab track demonstrator and transition zone

The test site is located on the Swedish heavy haul line *Malmbanan* in the passing siding at *Gransjö*, with coordinates of latitude 66.064 and longitude 21.407, see Figure 21(a). *Malmbanan* is a single-track railway line in the northern part of Sweden. Traffic is dominated by iron ore freight trains with axle loads 30 tonnes operating from the mines in *Kiruna* and *Malmberget* to the ports in *Narvik* (in Norway) and *Luleå*, see Figure 21(b). The speed of the loaded heavy haul trains is 60 km/h (70 km/h in tare conditions). In addition to iron ore trains, traffic consists of passenger trains at maximum speed 135 km/h and other types of freight trains. Nevertheless, the focus of the current study is on monitoring the response and performance of the track due to the loaded iron ore trains. The annual traffic load is around 15 MGT. The instrumented track section represents a transition between the conventional ballasted track and a 48 m field demonstrator section of a 3MB slab track. The 3MB demonstrator section at Gransjö was constructed in September 11 – 15, 2022 as part of the Horizon 2020 Shift2Rail EU project In2Track3. Under sleeper pads were implemented along 15 m (25 sleepers) of the ballasted track to reduce the stiffness gradient in the transition.



(a)



(b)

Figure 21. (a) An overview of the transition zone between ballasted track and 3MB slab track at Gransjö, north of Boden. (b) Geographical location of the iron ore line *Malmbanan*

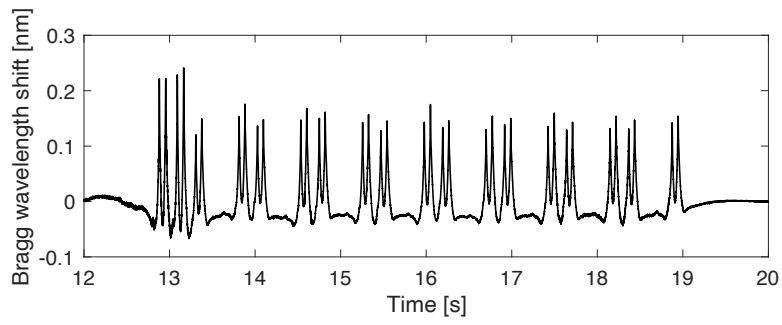
4.3 Fibre Bragg gratings

Fibre Bragg gratings (FBG) are periodic patterns of varying refractive index along the length of the core of an optical fibre, creating a fixed index modulation. At each periodic refraction index change, a small amount of light is reflected. All the reflected light signals combine coherently to one large reflection at a particular wavelength when the grating period is approximately half the wavelength of the light input. This is referred to as the Bragg condition, and the wavelength at which this reflection occurs is called the Bragg wavelength. Light signals at wavelengths other than the Bragg wavelength, which are not phase matched, are essentially transparent. Therefore, light propagates through the grating with negligible attenuation or signal variation. Only those wavelengths that satisfy the Bragg condition are affected and strongly back-reflected. The ability to accurately preset and maintain the grating wavelength is a fundamental feature and advantage of fibre Bragg gratings.

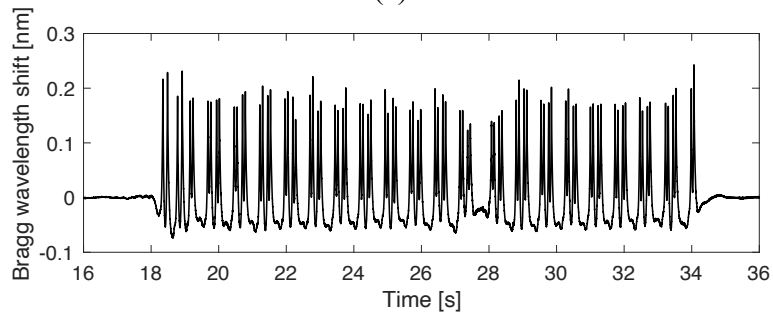
The central wavelength of the reflected component satisfies the Bragg relation $\lambda_{\text{Bragg}} = 2n\Lambda$, where n is the index of the refraction and Λ the period of the index of refraction variation of the FBG. Due to the temperature and strain dependence of the parameters n and Λ , the wavelength of the reflected component will also change as function of temperature and/or strain. This dependency is well known and allows determining the temperature or strain from the reflected FBG wavelength. A change of strain $\Delta\varepsilon$ and temperature ΔT will cause a wavelength shift $\Delta\lambda_B$ as in Eq. 5:

$$\Delta\lambda_B/\lambda_B = (1 - P_e) \Delta\varepsilon + (\alpha + \xi) \Delta T \quad \text{Eq. 5}$$

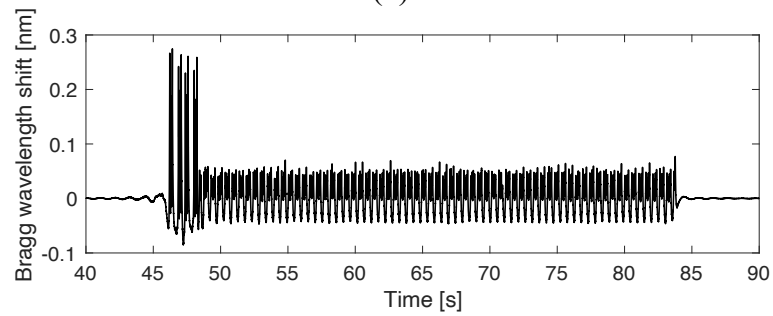
where P_e , α and ξ are the elastic-optical coefficient, the thermal expansion coefficient and the thermal-optical coefficient of the optical fibre, respectively. For four different trains passing the test site, Figure 22 shows examples of time histories of Bragg wavelength shifts from one sensor. Based on the number of axles, which is obtained by counting the total number of peaks in the Bragg wavelength shift signal, the vehicle type can be identified. Further, it can be clearly seen that the magnitude of the peaks shifts depending on the axle load. For example, the peaks for the loaded iron ore train in Figure 22(d) are six times higher than the peaks for the unloaded iron ore train in Figure 22(c). This is expected since the axle loads in loaded iron ore train is of the order 30 tonnes, while it is 5 tonnes for unloaded iron ore trains.



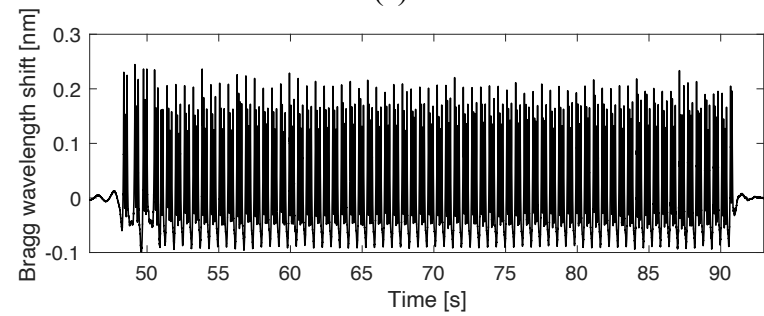
(a)



(b)



(c)



(d)

Figure 22. Time history of Bragg wavelength shift for (a) a passenger train, (b) a freight train, (c) an unloaded iron ore train, (d) a loaded iron ore train

4.4 Instrumentation

In this thesis, the instrumentation plan included sensors for the measurement of i) rail strains to assess rail bending moment and rail seat load; ii) vertical sleeper displacement; iii) vertical acceleration at sleeper end; iv) shear deformation of the rail to assess wheel load. An overview of the positioning of the sensors is shown in Figure 23. The setup includes four clusters placed at sections between two sleepers in sleeper bays 3, 5, 8, and 11 numbered from the transition. Each FBG-based cluster consists of one accelerometer, one displacement transducer, and one strain array including four strain gauges. One extra accelerometer was placed far from the transition and another one on the first block on the slab side. Four temporary electrical strain gauges bridge were added to measure wheel–rail contact forces. The permanent installation of sensor clusters is used for condition monitoring of the transition, whereas the temporary installation was used to monitor dynamic wheel–rail contact forces for a single train. In total, 30 FBG sensors were installed. Aluminium covers were added to protect the sensors and cables from mechanical damage and the harsh weather conditions.

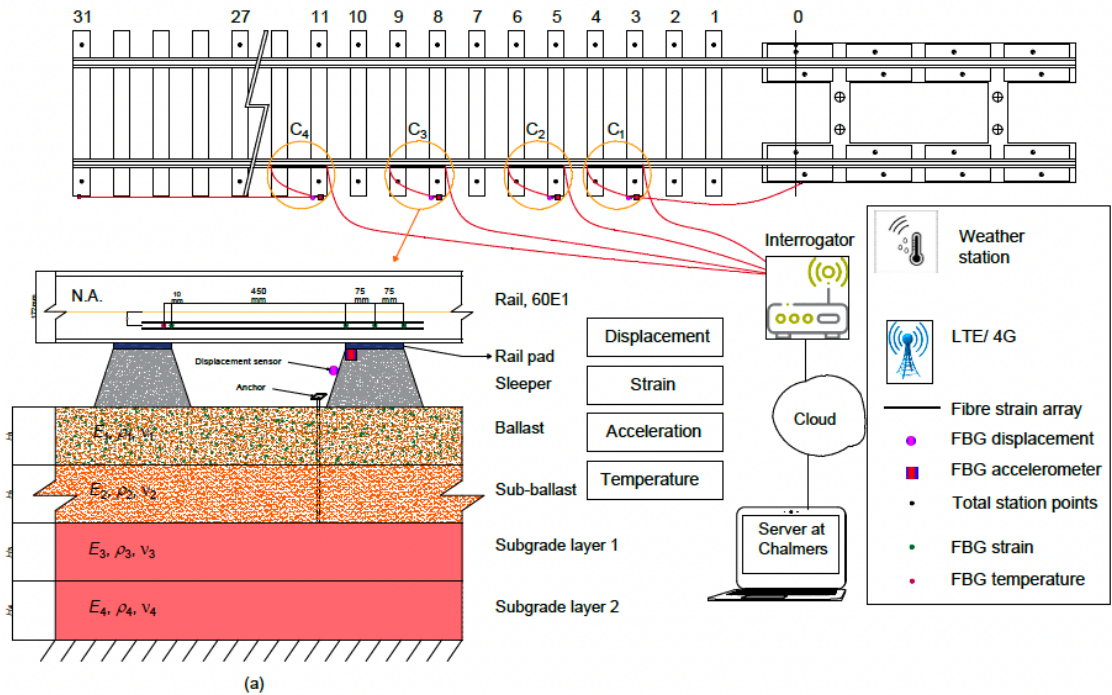


Figure 23. Schematic representation of the data acquisition system in a transition zone between ballasted track and 3MB slab track. The setup consists of four clusters (C1 – C4), each including a strain array (four strains on the rail web), a displacement transducer, and an accelerometer

Each strain array was welded at 31 mm below the neutral axis on one side of the rail to measure the magnitude of axial strain due to rail bending, see Figures 23 and 24. The rail surface was polished and dried before the installation. Strain sensors 1, 2 and 3 in each cluster were placed above a sleeper, while sensor 4 was located near the adjacent sleeper, see Figure 24. Due to the size of the displacement transducer and the limited available space, the transducer was positioned horizontally adjacent to the sleeper. Using a mechanism (L-shaped arm with a swivel and a roller), the downwards positive vertical displacement of the sleeper is converted to horizontal tension/compression of the displacement transducer, see Figure 25. Further, vertical accelerations were measured using six FBG-based accelerometers. Five of these were placed at the ends of sleepers 3, 5, 8, 11, and 31, while one was positioned on the first block on the slab track side. Wheel–rail contact force is a primary indicator of the dynamic vehicle–track interaction. In the current design for the monitoring setup, contact forces were considered complimentary to the condition monitoring setup using the FBG sensors. In addition to the installed instrumentation, a track geometry recording car has been used to measure vertical stiffness every 5 cm along the slab and transition zone, as well as for a quality controller of the longitudinal level of the track (not shown here). Further, the vertical settlement of several sleepers and the first block on the slab side have been measured on several occasions using a total station. Examples of results from the measurements will be presented in the sections below.

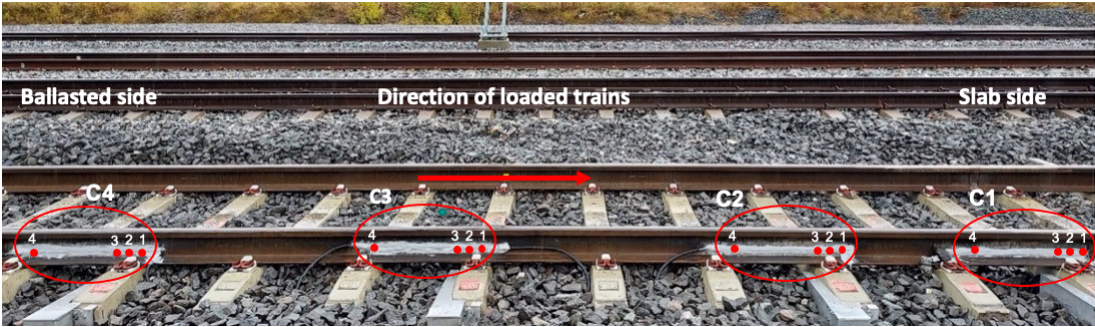


Figure 24. An overview of the four clusters (C1 – C4), and strain sensor numbering for each cluster



Figure 25. Detail of sleeper containing a vertical base plate, an L-shaped mechanism, one accelerometer and one displacement transducer. (a) The designed setup, (b) overview of an instrumented sleeper with an accelerometer and a displacement transducer. The positions of the anchor tip and the L-shaped mechanism with a swivel and a roller are shown

4.4.1 Rail strain and rail bending moment

The surface strain of a specimen can be measured by bonding an optical fibre with a fibre Bragg grating onto the surface. This requires a smooth surface. Furthermore, similar to when using a single electrical strain gauge, mechanically and thermally induced strains cannot be distinguished. Consequently, most FBG-based strain sensors have multiple gratings, *i.e.* one for strain sensing and one for temperature compensation. These sensors are packaged in a metal casing and can be directly mounted on the specimen by a fastener, spot welding or epoxy, which makes fibre handling easier and the sensor installation faster and more repeatable.

In the applied setup, strain and temperature are recorded in independent gratings. However, during a single train passage the temperature variation is negligible. Further, it can be argued that the applied data sampling (2 kHz) is higher than the frequency range of interest for the quasi-static rail bending due to the train loads and speeds in this trial [91]. In this thesis, the strain signals have been high-pass filtered at 1 Hz to adjust the baseline of the signal and prevent low frequency drift. The signals have also been detrended. In Figure 26, examples of rail strain above sleeper 11 due to the passing of different train types are depicted. By assuming Euler-Bernoulli beam theory for a known rail cross-section, and applying several sensors, the distribution of rail bending moment $M(x) = EI\epsilon(x)$ along the rail can be determined. For example, based on three sensors, time histories of the distribution of rail bending moment on top of four sleepers along the transition due to a loaded iron ore train is presented in Figure 27. This information can be used to detect the type of vehicle, train speed, and as an indication of the track support condition.

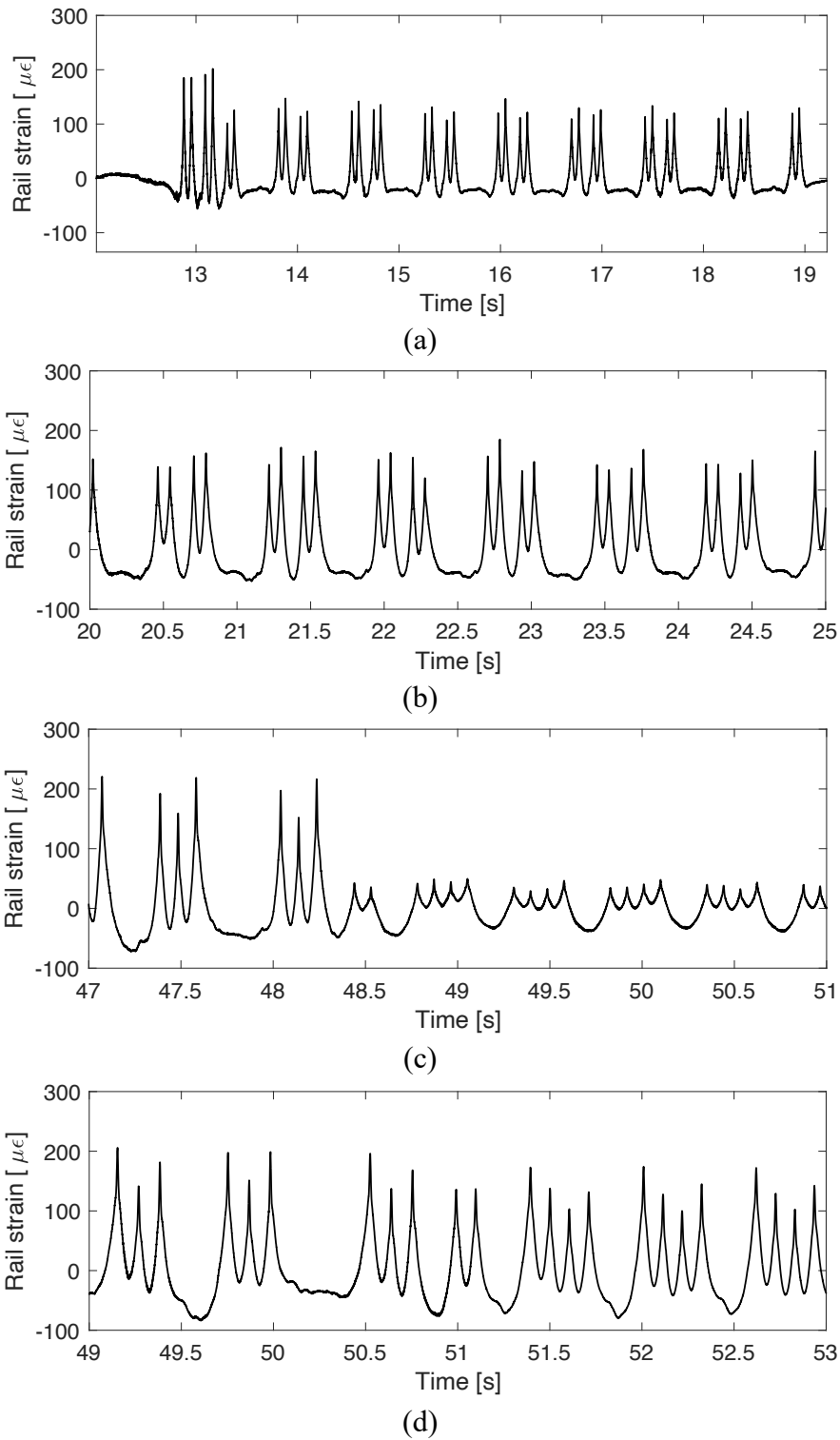


Figure 26. Time histories of high-pass filtered (1 Hz) rail strain above sleeper 11. (a) Passenger train, (b) freight train, (c) unloaded iron ore train, (d) loaded iron ore train

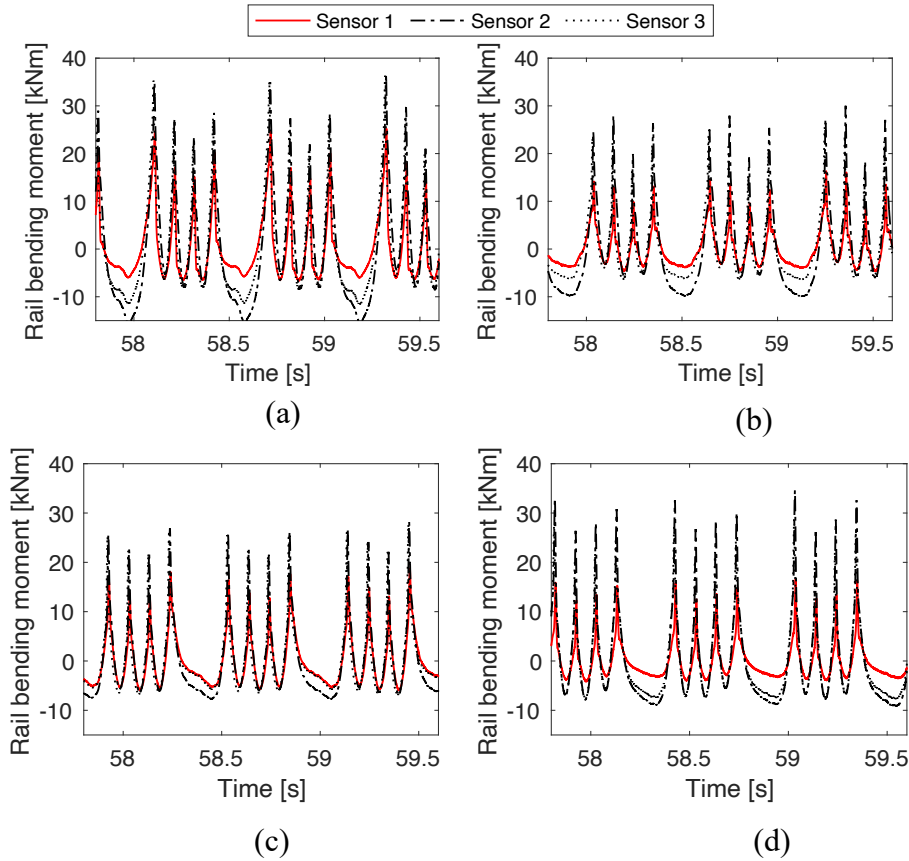
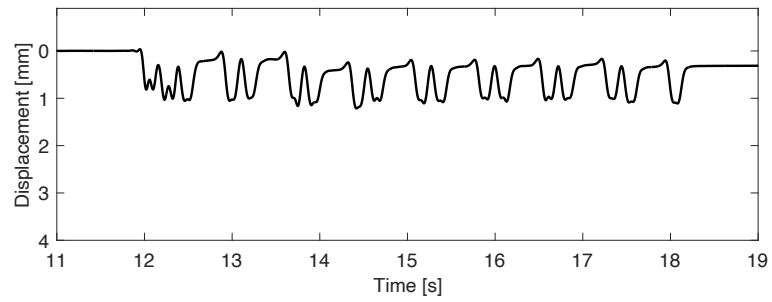


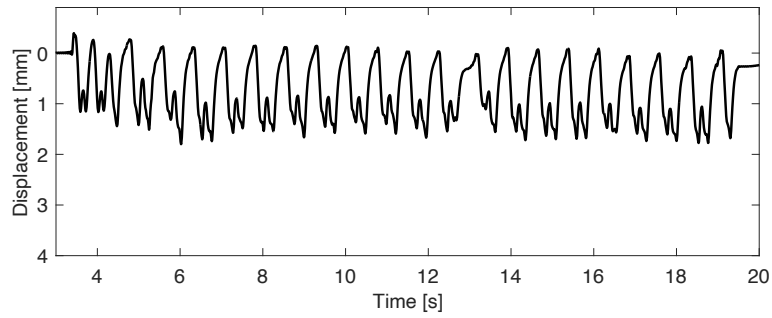
Figure 27. Time histories of rail bending moment above four sleepers along the transition due to a loaded iron ore train. (a) Sleeper 3, (b) sleeper 5, (c) sleeper 8, (d) sleeper 11. The loaded iron ore trains first pass over sensor 3, and then 2 and 1.

4.4.2 Vertical sleeper displacement and acceleration

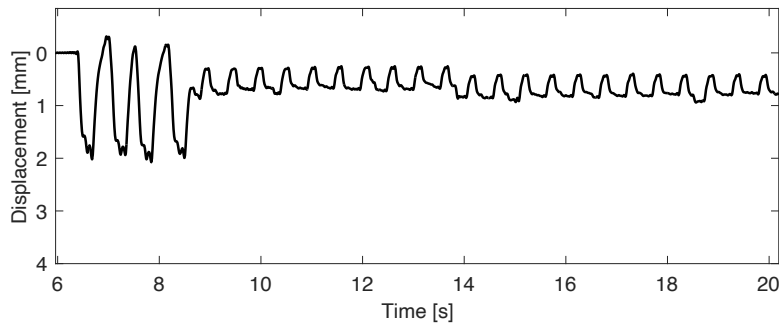
In this study, the 4th-order low-pass Butterworth filter with corner frequency 30 Hz has been applied to remove frequencies above those that are dominating the track bed movement. While the frequencies of interest may be up to about 30 Hz, data must be acquired at much greater acquisition rates to aid processing and eliminate noise and aliasing (here 2 kHz) [92]. The zero-phase digital filtering *filtfilt* is applied to preserve the phase shift in the signal. Examples of sleeper displacement are presented in Figure 28. Five of the FBG-based accelerometers were placed at sleeper ends 3, 5, 8, 11 and 31, while one was positioned on the first block on the slab track side. In this study, the recorded acceleration signals have been high-pass filtered at cut-off frequency 1 Hz based on recommendation from the provider of the sensor. Unfortunately, it was found that the signal-to-noise ratio in the measured acceleration on the sleepers was too low to obtain reasonable data for sleeper displacement reconstruction. However, this was not the case for the acceleration signal on the 3MB slab track side due to the higher mass of the slab track. In Figure 29, examples of signal from the accelerometer on the first block on the slab track side are depicted.



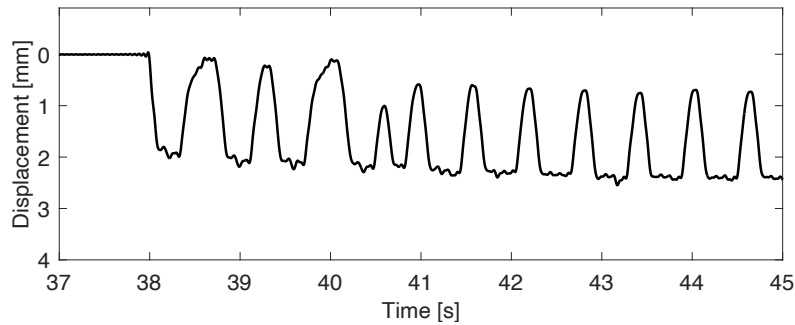
(a)



(b)

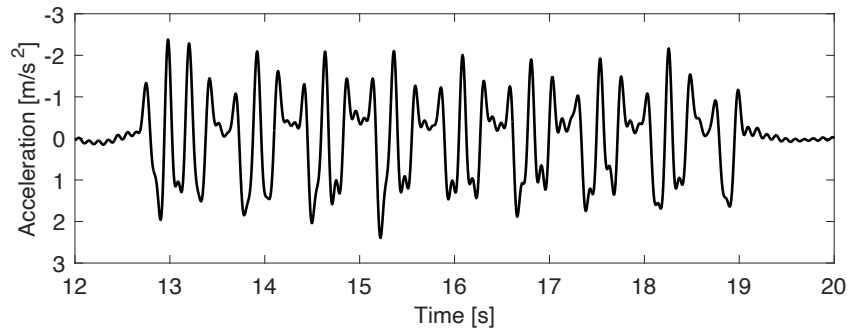


(c)

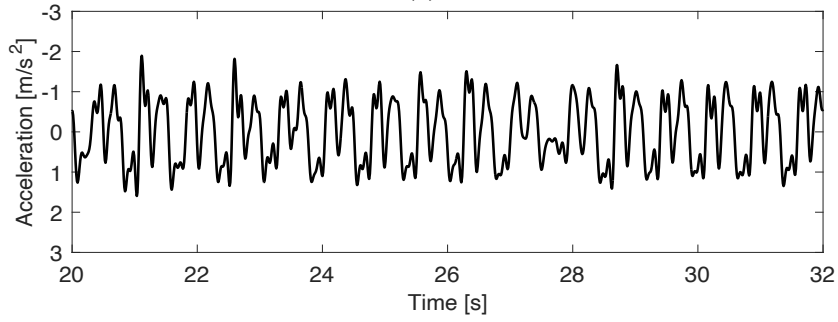


(d)

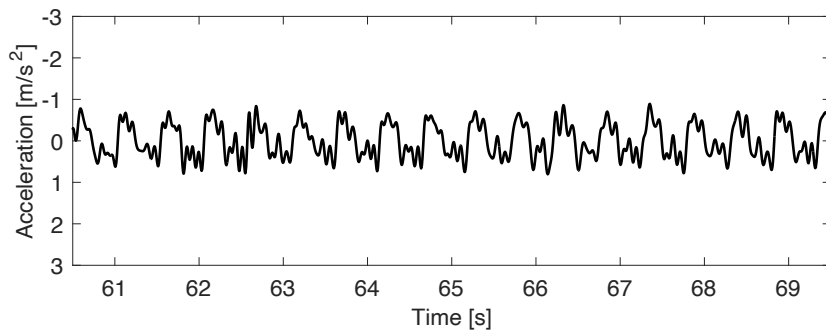
Figure 28. Time histories of sleeper displacement signal from sleeper 11. The signal has been low-pass filtered with frequency 30 Hz. (a) Passenger train, (b) freight train, (c) unloaded iron ore train, (d) loaded iron ore train. Displacement is presented relative to the displacement before the first axle in the first locomotive. Measurement from 2022-11-13



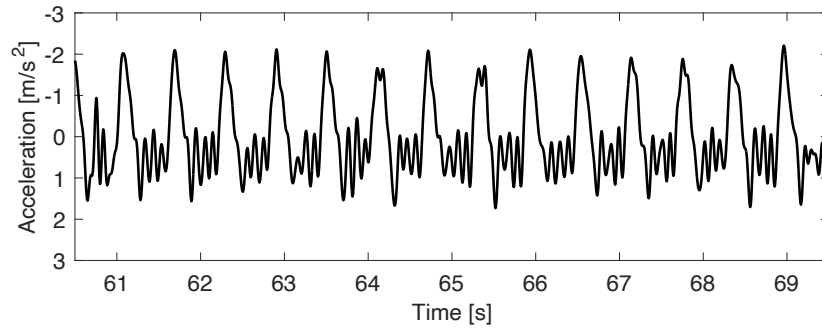
(a)



(b)



(c)



(d)

Figure 29. Time histories of sleeper acceleration signal from the first block on the slab track side. The signal has been band-pass filtered with cut-off frequencies at 1 and 30 Hz. (a) Passenger train, (b) freight train, (c) unloaded iron ore train, (d) loaded iron ore train. Measurement from 2022-11-13

4.4.3 Wheel–rail contact force

The vertical dynamic wheel–rail contact force has been measured in three sleeper bays using a standard configuration with two pairs of strain gauges mounted on the rail web at the neutral layer [93], see Figure 30. In this study, a half-bridge containing two waterproof strain gauges with sensing area of 6 mm × 2.2 mm were glued within a given span between two consecutive sleepers, and oriented at $\pm 45^\circ$ with respect to the horizontal and vertical coordinate system on the neutral axis of rail. Two extra half bridges were glued to the other side of the rail in sleeper bay number 3 to study any effects of transverse offset in the wheel load. A data logger fitted with full-bridge completion modules was used to sample the strain gauges at 10 kHz. Examples of results from the contact force measurement are presented in **Paper B**.



Figure 30. A full Wheatstone bridge mounted on the neutral axis of the rail web

4.4.4 Total station

A survey of sleeper levels was carried out using a Trimble S9 self-levelling, automatic tracking total station and active prism. The prism was placed in line with markings on each sleeper, and the total station was used to track and record the co-ordinates and height of the prism as it was moved sequentially from sleeper to sleeper along the track. The total station had an angular accuracy of 1 mm. The measured points are shown in Figure 23. Results from the total station survey are presented in **Paper B**.

5 Outline of the appended papers

5.1 Paper A

A methodology for the simulation of long-term differential track settlement, the development of voided sleepers, and the evolving irregularity in vertical track geometry at a transition between a ballasted track and 3MB slab track is presented. For a prescribed traffic load, the accumulated settlement is predicted using an iterative approach. It is based on a time-domain model of vertical dynamic vehicle–track interaction to calculate the contact forces between sleepers and ballast in the short term. These are used in an empirical model to determine the settlement of the ballast/subgrade below each sleeper in the long term. For heavy haul traffic, the simulation procedure has been applied for the transition zone at Gransjö, and it is demonstrated by investigating the influence of higher axle loads and the implementation of USPs. It is shown that the distribution of forces transmitted to the ballast varies along a transition zone. This is due to the stiffness gradient at the transition, but even more so should there be a misalignment in vertical rail level, for example, due to a densification of ballast after the first few load cycles. In both cases, a transient pitching motion of the passing vehicles is generated leading to a contribution to the dynamic loading resulting in a local maximum in settlement at sleepers near the transition. The use of USPs reduces track stiffness at rail level and leads to a wider distribution of load and reduced settlement along the track.

5.2 Paper B

A field instrumentation set-up for real-time condition monitoring has been developed to assess the influence of traffic load on accumulated settlement in the transition zone between 3MB slab track and ballasted track in the In2Track3 demonstrator at Gransjö on Malmbanan. The instrumentation comprises four clusters, each with an optical strain gauge array in the rail web, an accelerometer on the sleeper end, and a displacement transducer on the sleeper end. The setup was installed simultaneously with the 3MB slab track. Condition monitoring of the transition zone commenced immediately after the construction in September 2022. The early measurements (until January 2022) have been used for calibrating and evaluating the set-up for measuring the dynamic response and permanent deformation of the track system during the passage of individual loaded iron ore trains. These continuous measurements enable to quantify the evolving changes in the transition zone in terms of vertical wheel–rail contact force, rail bending moment, sleeper displacement, and sleeper acceleration. The aim of the field test at Gransjö is to verify and calibrate a numerical model for prediction of long-term differential settlement in a transition zone.

References

- [1] Indraratna B, Babar Sajjad M, Ngo T, Gomes Correia A, Kelly R. Improved performance of ballasted tracks at transition zones: A review of experimental and modelling approaches. *Transportation Geotechnics* 2019; 21:100260.
- [2] Grossoni I, Hawksbee S, Jorge P, Bezin Y, Magalhaes H. Prediction of track settlement at high-speed railway transitions between embankment and bridge in the proximity of a turnout. *Transportation Geotechnics* 2022; 37:100879.
- [3] Sakhare A, Farooq H, Nimbalkar S, Dodagoudar GR. Dynamic behavior of the transition zone of an integral abutment bridge. *Sustainability* 2022; 14:1–18.
- [4] Ramos A, Gomes Correia A, Calçada R, Connolly DP. Ballastless railway track transition zones: An embankment to tunnel analysis. *Transportation Geotechnics* 2022:100728.
- [5] Ramos A, Gomes Correia A, Calçada R, Alves Costa P, Esen A, Woodward PK, et al. Influence of track foundation on the performance of ballast and concrete slab tracks under cyclic loading: Physical modelling and numerical model calibration. *Journal of Construction and Building Materials* 2021; 277:122245.
- [6] Aggestam E, Nielsen JCO. Multi-objective optimisation of transition zones between slab track and ballasted track using a genetic algorithm. *Journal of Sound and Vibration* 2019; 446:91–112.
- [7] Varandas JN, Paixão A, Fortunato E. A study on the dynamic train-track interaction over cut-fill transitions on buried culverts. *Computers and Structures* 2017; 189:49–61.
- [8] Paixão A, Varandas JN, Fortunato E. Dynamic behavior in transition zones and long-term railway track performance. *Frontiers in Built Environment* 2021; 7:1–16.
- [9] Varandas JN, Hölscher P, Silva MAG. Settlement of ballasted track under traffic loading: Application to transition zones. *Proceedings of the Institution of Mechanical Engineers, Part F: Journal of Rail and Rapid Transit* 2014;228:242–59.
- [10] Sañudo R, Dell’Olio L, Casado JA, Carrascal IA, Diego S. Track transitions in railways: A review. *Construction and Building Materials* 2016; 112:140–57.
- [11] Shan Y, Zhou S, Wang B, Ho CL. Differential settlement prediction of ballasted tracks in bridge–embankment transition zones. *Journal of Geotechnical and Geoenvironmental Engineering* 2020; 146:1–18.
- [12] Wang H, Markine V. Modelling of the long-term behaviour of transition zones: Prediction of track settlement. *Engineering Structures* 2018; 156:294–304.
- [13] Fortunato E, Paixão A, Calçada R. Railway track transition zones: Design, construction, monitoring and numerical modelling. *International Journal of Railway Technology* 2013; 2:33–58.

- [14] Tutumluer E, Stark TD, Mishra D, Hyslip JP. Investigation and mitigation of differential movement at railway transitions for US high speed passenger rail and joint passenger/freight corridors. Joint Rail Conference, JRC 2012 2012:75–84.
- [15] Sañudo R, Cerrada M, Alonso B, Dell’Olio L. Analysis of the influence of support positions in transition zones. A numerical analysis. *Journal of Construction and Building Materials* 2017; 145:207–17.
- [16] Sasaoka CD, Davis DD, Koch K, Reiff RP. Implementing track transition solutions. *Technology Digest TD-05-001* 2005.
- [17] Karlsson R. Tekniska systemkrav för Ostlänken (Technical system requirements for Ostlänken, in Swedish), Trafikverket. vol. 1v2.0. 2014.
- [18] Shahraki M, Warnakulasooriya C, Witt KJ. Numerical study of transition zone between ballasted and ballastless railway track. *Transportation Geotechnics* 2015; 3:58–67.
- [19] Selig ET, Waters JM. *Track Geotechnology and Substructure Management*. London: Thomas Telford; 1994.
- [20] Li D, Selig ET. Method for railroad track foundation design. Development. *Journal of Geotechnical and Geoenvironmental Engineering* 1998; 124:316–22.
- [21] Dahlberg T. Some railroad settlement models - A critical review. *Proceedings of the Institution of Mechanical Engineers, Part F: Journal of Rail and Rapid Transit* 2001;215:289–300.
- [22] Esveld C. *Modern railway track, MRT-productions, Zaltbommel*. 2001.
- [23] Li D, Hyslip J, Sussmann T, Chrismer S. *Substructure from: Railway Geotechnics* CRC Press. 2002.
- [24] Aggestam E, Nielsen JCO, Bolmsvik R. Simulation of vertical dynamic vehicle–track interaction using a two-dimensional slab track model. *Vehicle System Dynamics* 2018; 56:1633–57.
- [25] Morales-Gamiz FJ. Design requirements, concepts, and prototype test results for new system of ballastless system (3MB slab track), Capacity for rail; Deliverable 11.3. 2017.
- [26] Wang H, Markine V, Liu X. Experimental analysis of railway track settlement in transition zones. *Proceedings of the Institution of Mechanical Engineers, Part F: Journal of Rail and Rapid Transit* 2018;232:1774–89.
- [27] Namura A, Suzuki T. Evaluation of countermeasures against differential settlement at track transitions. *Quarterly Report of RTRI (Railway Technical Research Institute, Japan)* 2007; 48:176–82.

- [28] Shan Y, Zhou S, Wang B, Ho CL. Differential settlement prediction of ballasted tracks in bridge–embankment transition zones. *Journal of Geotechnical and Geoenvironmental Engineering* 2020; 146:04020075.
- [29] Peduto D, Giangreco C, Venmans AAM. Differential settlements affecting transition zones between bridges and road embankments on soft soils: Numerical analysis of maintenance scenarios by multi-source monitoring data assimilation. *Transportation Geotechnics* 2020; 24:100369.
- [30] Charoenwong C, Connolly DP, Woodward PK, Galvín P, Alves Costa P. Numerical modelling of the evolution of differential settlement of railway tracks. *Eleventh International Conference on the Bearing Capacity of Roads, Railways and Airfields* 2022;3:291–300.
- [31] Nielsen JCO, Li X. Railway track geometry degradation due to differential settlement of ballast/subgrade – Numerical prediction by an iterative procedure. *Journal of Sound and Vibration* 2018; 412:441–56.
- [32] Li X, Ekh M, and Nielsen JCO. Three-dimensional modelling of differential railway track settlement using a cycle domain constitutive model. *International Journal for Numerical and Analytical Methods in Geomechanics* 2016; 30:1303–36.
- [33] Guo Y, Zhai W. Long-term prediction of track geometry degradation in high-speed vehicle–ballastless track system due to differential subgrade settlement. *Soil Dynamics and Earthquake Engineering* 2018; 113:1–11.
- [34] Nicks JE. The bump at the end of the railway bridge. PhD Thesis. Texas A&M University, Texas, United States, 2009.
- [35] Zaman BM, Gopalasingam A, Member A, Laguros JG. Consolidation settlement of bridge approach foundation. *Journal of Geotechnical Engineering* 1991; 117:219–40.
- [36] Long JH, Olson SM, Stark TD, Samara EA. Differential movement at embankment-bridge structure interface in Illinois. *Transportation Research Record* 1998:53–60.
- [37] Wheeler LN, Andy Take W, Hoults NA, Le H. Use of fiber optic sensing to measure distributed rail strains and determine rail seat forces under a moving train. *Canadian Geotechnical Journal* 2019; 56:1–13.
- [38] Li M. Simulations of the vertical track stiffness and its variations for slab track along transition zones, Trafikverket. 2018.
- [39] Le Pen L, Milne D, Thompson D, Powrie W. Evaluating railway track support stiffness from trackside measurements in the absence of wheel load data. *Canadian Geotechnical Journal* 2016; 53:1156–66.
- [40] Dahlberg T. Railway track stiffness variations - Consequences and countermeasures. *International Journal of Civil Engineering* 2010; 8:1–12.

- [41] Berggren E. Railway track stiffness dynamic measurements and evaluation for efficient maintenance. PhD Thesis, KTH, Stockholm, Sweden. 2009.
- [42] Nielsen J. Optimum vertical track stiffness. Research Report 2010:11, Department of Applied Mechanics, Chalmers University of Technology, Göteborg, Sweden 2010: 2010.
- [43] CEN. Railway applications – Ballastless track systems – Part 1: General requirements, FprEN 16342-1. 2017.
- [44] Wang H, Markine V. Dynamic behaviour of the track in transition zones considering the differential settlement. *Journal of Sound and Vibration* 2019; 459:114863.
- [45] Namura A, Kohata Y, Miura S. Effect of sleeper size on ballasted track settlement. *Quarterly Report of RTRI (Railway Technical Research Institute, Japan)* 2004; 45:156–61.
- [46] Chumyem P, Connolly DP, Woodward PK, Markine V. The effect of soil improvement and auxiliary rails at railway track transition zones. *Soil Dynamics and Earthquake Engineering* 2022; 155:107200.
- [47] Paixão A, Varandas JN, Fortunato E, Calçada R. Numerical simulations to improve the use of under sleeper pads at transition zones to railway bridges. *Engineering Structures* 2018; 164:169–82.
- [48] Insa R, Salvador P, Inarejos J, Roda A. Analysis of the influence of under sleeper pads on the railway vehicle/track dynamic interaction in transition zones. *Proceedings of the Institution of Mechanical Engineers, Part F: Journal of Rail and Rapid Transit* 2012;226:409–20.
- [49] Alves Ribeiro C, Paixão A, Fortunato E, Calçada R. Under sleeper pads in transition zones at railway underpasses: numerical modelling and experimental validation. *Structure and Infrastructure Engineering* 2015; 11:1432–49.
- [50] Le Pen L, Watson G, Hudson A, Powrie W. Behaviour of under sleeper pads at switches and crossings – Field measurements. *Proceedings of the Institution of Mechanical Engineers, Part F: Journal of Rail and Rapid Transit* 2018;232:1049–63.
- [51] Abadi T, Pen L Le, Zervos A, Powrie W. Effect of sleeper interventions on railway track performance. *Journal of Geotechnical and Geoenvironmental Engineering* 2019; 145:04019009.
- [52] Li H, McDowell GR. Discrete element modelling of under sleeper pads using a box test. *Granular Matter* 2018; 20:1–12.
- [53] Puppala A, Saride S, Archeewa E, Hoyos L, Nazarian S. Recommendations for design, construction, and maintenance of bridge approach slabs, technical report 0-6022-1, Department of civil engineering, the university of Texas at Arlington, Arlington, Texas. 2008.

- [54] Jing G, Qie L, Markine V, Jia W. Polyurethane reinforced ballasted track: Review, innovation and challenge. *Construction and Building Materials* 2019; 208:734–48.
- [55] Sehgal L, Garg A, Sehgal V, Buttlar W. Hot mix asphalt in ballasted railway track: International experience and inferences. In *Proceedings of the Institution of Permanent Way Engineers (IPWE) International Technical Seminar 2017*:1–12.
- [56] Coelho B, Hölscher P, Priest J, Powrie W, Barends F. An assessment of transition zone performance. *Proceedings of the Institution of Mechanical Engineers, Part F: Journal of Rail and Rapid Transit* 2011;225:129–39.
- [57] Fara A. Transition zones for railway bridges - A study of the Sikån bridge. MSc Thesis. Luleå University of Technology, Department of Civil, Environmental, and Natural Resources Engineering, Luleå, Sweden. 2014.
- [58] Li D, Davis D. Transition of railroad bridge approaches. *Journal of Geotechnical and Geoenvironmental Engineering* 2005; 131:1392–8.
- [59] Paixão A. Transition zones in railway tracks: An experimental and numerical study on the structural behaviour. PhD Thesis. Faculty of Engineering, University of Porto, Porto, Portugal 2014.
- [60] Rose JG, Stark TD, Wilk ST, Purcell M. Design and monitoring of well-performing bridge transitions. *Joint Rail Conference, JRC 2015* 2015:1–9.
- [61] Suiker ASJ, de Borst R. A numerical model for the cyclic deterioration of railway tracks. *International Journal for Numerical Methods in Engineering* 2003; 57:441–70.
- [62] Vizcarra GC, Nimbalkar S, Casagrande M. Modeling behaviour of railway ballast in prismatic apparatus using discrete element method. *Procedia Engineering* 2016; 143:1177–84.
- [63] Yu Z, Connolly DP, Woodward PK, Laghrouche O. Settlement behaviour of hybrid asphalt-ballast railway tracks. *Construction and Building Materials* 2019; 208:808–17.
- [64] Abadi T, Le Pen L, Zervos A, Powrie W. A review and evaluation of ballast settlement models using results from the Southampton Railway Testing Facility (SRTF). *Procedia Engineering* 143;2016: 999–1006.
- [65] Grossoni I, Powrie W, Zervos A, Bezin Y, Le Pen L. Modelling railway ballasted track settlement in vehicle-track interaction analysis. *Transportation Geotechnics* 2021; 26:100433.
- [66] Knothe K, Grassie SL. Modelling of railway track and vehicle/track interaction at high frequencies, *Vehicle System Dynamics: International Journal of Vehicle Mechanics and Mobility* 1993;22: 209-262.

- [67] Connolly DP, Kouroussis G, Laghrouche O, Ho CL, Forde MC. Benchmarking railway vibrations - Track, vehicle, ground and building effects. *Construction and Building Materials* 2015; 92:64–81.
- [68] Lamprea-Pineda AC, Connolly DP, Hussein MFM. Beams on elastic foundations – A review of railway applications and solutions. *Transportation Geotechnics* 2022; 33:100696.
- [69] Nielsen JCO, Igeland A. Vertical dynamic interaction between train and track— influence of wheel and track imperfections. *Journal of Sound and Vibration* 1995; 187:825–39.
- [70] Kouroussis G, Connolly DP, Verlinden O. Railway-induced ground vibrations – A review of vehicle effects. *International Journal of Rail Transportation* 2014; 2:69–110.
- [71] Krzyżyński T. On continuous subsystem modelling in the dynamic interaction problem of train-track-system. *Vehicle System Dynamics* 1995; 24:311–24.
- [72] Lei X, Mao L. Dynamic response analyses of vehicle and track coupled system on track transition of conventional high-speed railway. *Journal of Sound and Vibration* 2004; 271:1133–46.
- [73] Dahal B, Mishra D. Discrete element modeling of permanent deformation accumulation in railroad ballast considering particle breakage. *Frontiers in Built Environment* 2020; 5:1–14.
- [74] Chen C, McDowell GR. An investigation of the dynamic behaviour of track transition zones using discrete element modelling. *Proceedings of the Institution of Mechanical Engineers, Part F: Journal of Rail and Rapid Transit* 2016;230:117–28.
- [75] Shi C, Zhao C, Zhang X, Andersson A. Analysis on dynamic performance of different track transition forms using the discrete element/finite difference hybrid method. *Computers and Structures* 2020; 230:106187.
- [76] Zuada Coelho B, Varandas JN, Hijma MP, Zoeteman A. Towards network assessment of permanent railway track deformation. *Transportation Geotechnics* 2021;29.
- [77] Wolf JP, Deeks AJ. *Foundation vibration analysis: a strength-of-materials approach*. Elsevier 2004; 42:218.
- [78] Suiker ASJ, Selig ET, Frenkel R. Static and cyclic triaxial testing of ballast and subballast. *Journal of Geotechnical and Geoenvironmental Engineering* 2005; 131:771–82.
- [79] Shenton MJ. Deformation of railway ballast under repeated loading conditions. *Railroad Track Mechanics and Technology* 1978:405–25.
- [80] Iwnicki S, Grassie S, Kik W. Track settlement prediction using computer simulation tools. *Vehicle System Dynamics* 2000; 33:37–46.

- [81] Abadi TC. Effect of sleeper and ballast interventions on rail track performance, PhD Thesis. Faculty of Engineering and the Environment, University of Southampton, Southampton, England. 2015.
- [82] Lakusic S, Ahac M, Haladin I, Lakušič S, Ahac M, Haladin I. Experimental investigation of railway track with under sleeper pad. Proceedings of the 10th Slovenian Road and Transportation Congress 2010:386–393.
- [83] Ng CWW, Zhou C, Yuan Q, Xu J. Resilient modulus of unsaturated subgrade soil: Experimental and theoretical investigations. Canadian Geotechnical Journal 2013; 50:223–32.
- [84] Li BD, Selig ET. Resilient modulus for fine-grained subgrade soils. Journal of Geotechnical Engineering 1994; 120:939–57.
- [85] Indraratna B, Nimbalkar S. Stress-strain degradation response of railway ballast stabilized with geosynthetics. Journal of Geotechnical and Geoenvironmental Engineering 2013; 139:684–700.
- [86] Sato Y. Japanese studies on deterioration of ballasted track. Vehicle System Dynamics 1995; 24:197–208.
- [87] Saussine G, Quezada JC, Breul P, Radjai F. Railway ballast settlement: A new predictive model. Civil-Comp Proceedings 2014; 104:1–12.
- [88] Banimahd M. Advanced finite element modelling of coupled train-track systems: A geotechnical perspective. PhD Thesis. Heriot-Watt University; School of the Built Environment; Edinburgh; Scotland 2008.
- [89] Sayeed MA, Shahin MA. Design of ballasted railway track foundations using numerical modelling. Part I: Development. Canadian Geotechnical Journal 2018; 55:353–68.
- [90] Milne D, Harkness J, Le Pen L, Powrie W. The influence of variation in track level and support system stiffness over longer lengths of track for track performance and vehicle track interaction. Vehicle System Dynamics 2021; 59:245–68.
- [91] Thompson D. Railway noise and vibration: Mechanisms, modelling and means of control, Elsevier. Southampton, UK: 2009.
- [92] Powrie W, Le Pen L, Milne D, Watson G, Harkness J. Behaviour of under-track crossings on ballasted railways. Transportation Geotechnics 2019; 21:100258.
- [93] Mishra D, Tutumluer E, Boler H, Hyslip JR, Sussmann TR. Railroad track transitions with multidepth deflectometers and strain gauges. Transportation Research Record 2014; 2448:105–14.

